Supplementary Information (SI) for Chemical Science.
This journal is © The Royal Society of Chemistry 2024

Supporting Information

Revisiting a Classic Carbocation – DFT, Coupled-Cluster, and *ab initio* Molecular Dynamics Computations on Barbaralyl Cation Formation and Rearrangements

Wentao Guo,[‡] Wang-Yeuk Kong,[‡] Dean J. Tantillo*

Table of Contents

Computational details

Initial geometry optimization and vibrational analysis were performed with the Gaussian 16 Revision C.01 suite of programs utilizing the M06-2X functional with Aldrich's split valance polarized basis sets (def2-SVP) for all atoms in gas phase.[1,2] Single point energy corrections were then computed at the DLPNO-CCSD(T)/CBS level of theory using ORCA 5.0.4.[3–5] Basis set extrapolation to the complete basis set (CBS) limit was performed by focal point analysis with def2-TZVPP and def2-QZVPP basis sets.[2] The TightPNO cutoff was employed throughout the local coupled cluster calculations.[5] Quasi-harmonic thermochemical corrections at -135 °C (138.15 K) and 1.0 M concentration were obtained using the GoodVibes package.[6] With this approach, the transition structure (**TS2**) corresponding to the **A** to **A** interconversion was not located, yet this TS was reported previously.[7,8] After extensive benchmarking, we used CAM-B3LYP/6-31G(d) geometries throughout.[9,10]

Transition structures were verified to process only one vibrational mode with imaginary frequency and by subsequent intrinsic reaction coordinate (IRC) calculations.[11] Data set collection of optimized geometries are available at the ioChem-BD repository *via* https://doi.org/10.19061/iochem-bd-6-371 (benchmarking results) and https://doi.org/10.19061/iochem-bd-6-375 (key structures).[12]

Benchmark

Benchmarks herein use geometry optimized at ωB97X-D/def2-TZVP level of theory as all TS/minima previously reported for the barbaralyl cation could be optimized at this level. As we aim to find a level for AIMD simulation, we opted for 6-31G(d) and def2-SVP basis sets which are computationally efficient.[13]

We first benchmarked against relative electronic energies obtained at DLPNO-CCSD(T)/CBS level of theory against various exchange-correlation functionals in conjunction with 6-31G(d) and def2-SVP. The results are summarized below.

Relative Electronic Energies

To identify the optimal level of theory, we benchmarked the relative energies of all stationary points against the energy of structure **A**, which was found to be the lowest-energy structure for the barbaralyl cation. The reference relative energies obtained using DLPNO-CCSD(T)/CBS are summarized in Table S1. The results including mean absolute error (MAE) for the 39 density functionals with the 6-31G(d) and def2-SVP basis sets are presented in Tables S2 and S3, respectively.

Table S1. Relative potential energy relative to **A** under CCSD(T)/CBS level of theory in kcal/mol.

	A	***B***	***TS2***	***TS3***	***TS4***
DLPNO-CCSD(T)	0.00	3.06	2.66	4.23	5.41

6-31G(d) Basis Set

Table S2. Benchmarking result using 6-31G(d) basis set in kcal/mol.

	A	***B***	***TS2***	***TS3***	***TS4***	*MAE*
APFD[14]	0.00	-1.92	2.76	0.59	7.94	2.81
B1B95[15]	0.00	-2.69	3.37	0.02	9.02	3.57
B1LYP[16]	0.00	3.00	0.91	4.04	3.58	0.96
B3LYP[16]	0.00	1.81	0.85	3.07	4.09	1.39
B3PW91[17]	0.00	-1.92	2.42	0.47	7.51	2.77
B97-D3[18,19]	0.00	-0.25	-0.55	1.97	3.61	2.65
BH&HLYP[20]	0.00	6.20	2.47	6.98	3.70	1.95
BLYP[21–23]	0.00	0.56	-0.64	1.69	3.07	2.67
BMK[24]	0.00	2.60	2.52	1.55	6.99	1.22
CAM-B3LYP[10]	0.00	3.18	2.65	4.58	5.22	0.17
B3LYP-D3(BJ)[13,18]	0.00	2.51	0.24	3.84	3.40	1.34
BLYP-D3(BJ)[13,21–23]	0.00	1.42	-1.38	2.63	2.24	2.62
CAM-B3LYP-D3(BJ)[10,18]	0.00	3.56	2.36	4.98	4.83	0.53
PBE0-D3(BJ)[13,25]	0.00	-2.15	2.89	0.58	8.24	2.98
PBE-D3(BJ)[18,26]	0.00	-4.44	1.31	-1.62	7.65	4.23
HSEH1PBE[27]	0.00	-2.28	3.00	0.37	8.21	3.09
LC-ωHPBE[28,29]	0.00	0.14	6.50	3.12	10.15	3.15
M06[1]	0.00	-3.31	4.53	0.50	8.66	3.81
M06-2X[1]	0.00	-0.78	4.66	1.61	8.56	2.90

M06-L[30]	0.00	-6.24	4.37	-1.92	9.64	5.35
M11[31]	0.00	-0.72	5.53	1.25	9.71	3.48
MN12-L[32]	0.00	-0.94	1.52	1.62	6.16	2.13
MN12-SX[33]	0.00	0.04	2.28	1.96	6.47	1.69
MN15[34]	0.00	0.40	3.01	2.54	7.68	1.74
N12-SX[33]	0.00	-3.30	3.36	-0.49	8.88	3.81
O3LYP[35,36]	0.00	-3.23	2.43	-0.47	7.58	3.35
PBE0[25]	0.00	-2.54	3.19	0.16	8.63	3.35
PBE[26]	0.00	-4.85	1.66	-2.06	8.05	4.46
PBEh1PBE[25]	0.00	-2.27	3.14	0.40	8.33	3.14
PW6B95-D3[37]	0.00	-1.05	2.60	1.23	7.55	2.33
SOGGA11X[38]	0.00	1.05	3.67	3.18	6.98	1.41
TPSS[39]	0.00	-3.51	1.66	-1.04	7.51	3.73
TPSSh[40]	0.00	-2.71	2.27	-0.25	7.79	3.26
X3LYP[40]	0.00	1.94	0.97	3.20	4.18	1.27
mPW1PW91[41]	0.00	-1.76	2.87	0.69	7.96	2.78
revTPSS[42,43]	0.00	-4.48	2.10	-1.79	8.75	4.36
τ-HCTH hyb[38,44].	0.00	-0.07	1.10	1.18	5.74	2.02
ωB97X[45]	0.00	2.00	4.89	4.22	7.17	1.26
ωB97X-D[13]	0.00	1.58	3.14	3.17	6.42	1.01

To compare the accuracy of different levels of theory, the mean absolute error, taking CCSD(T)/CBS as the standard, is visualized in Figure S1 below. CAM-B3LYP outperforms the other 38 functionals in the specific case of the barbaralyl cation. In contrast, M06-2X, which has been widely used in carbocation calculations, gives a relatively large deviation from the reference value.

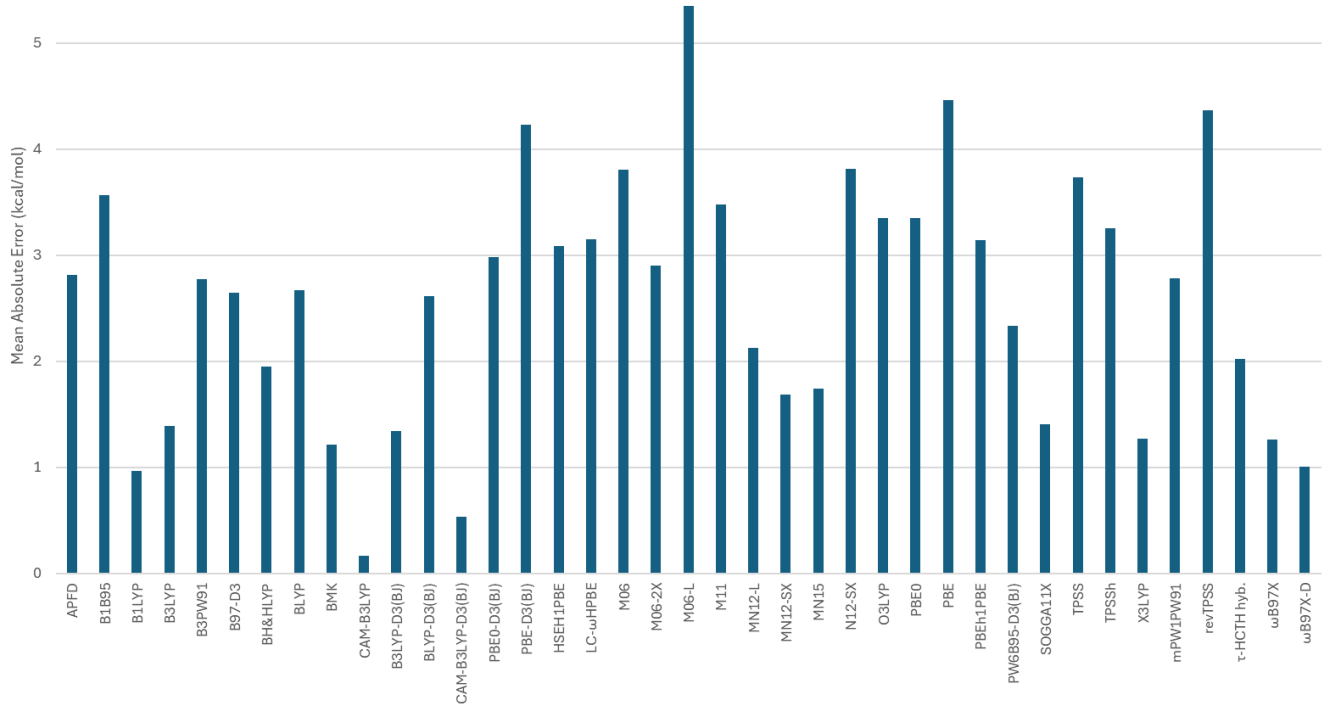

Figure S1. Mean absolute error (MAE) values for benchmarking functionals using the 6-31G(d) basis set, relative to the CCSD(T)/CBS reference energies in kcal/mol. The CAM-B3LYP functional exhibits the lowest MAE for the barbaralyl cation system.

Additionally, we compared the energy of structure **B** relative to structure **A**, which are the two minimum energy structures of the barbaralyl cation. As shown in Figure S2, the reference level CCSD(T)/CBS indicates that structure B is 2.6 kcal/mol higher in energy than structure A. Among the 39 density functionals tested, only 6 functionals correctly predicted that structure B is more than 2 kcal/mol higher in energy than structure A.

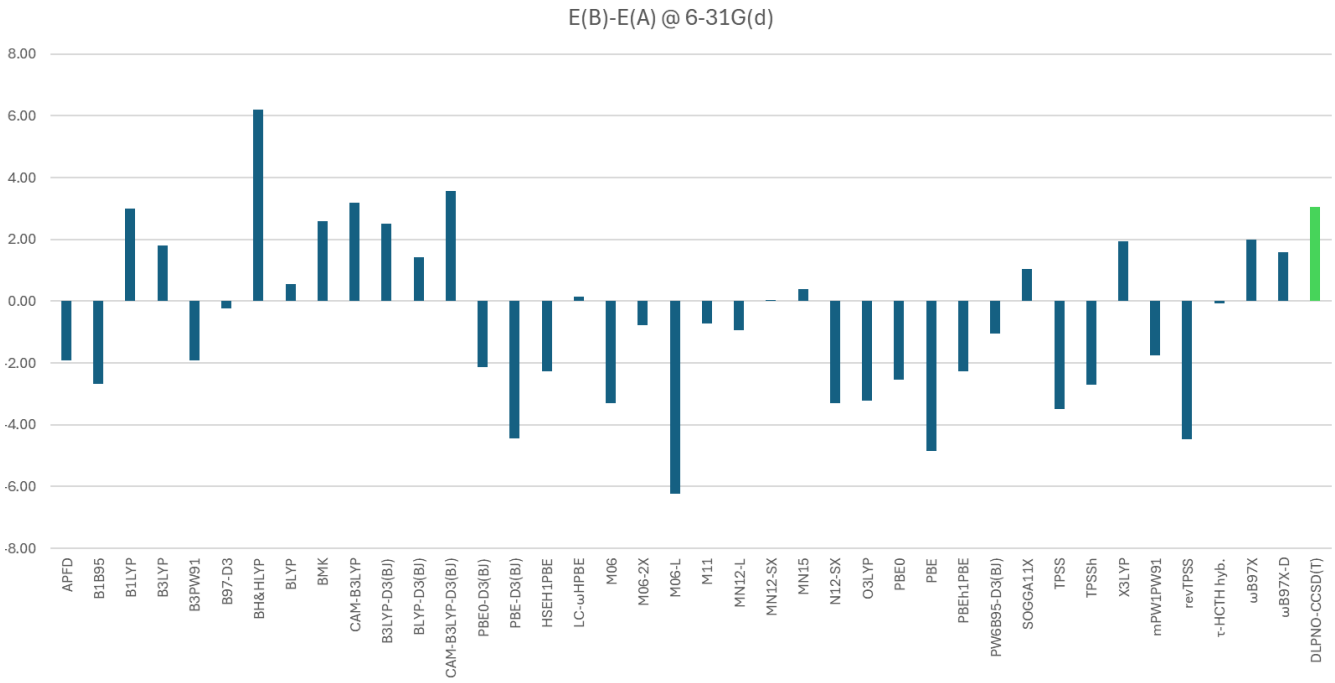

Figure S2. Relative energy of **B** (kcal/mol) for benchmarking functionals using the 6-31G(d) basis set, relative to the CCSD(T)/CBS reference energies in kcal/mol. The reference result is highlighted in green.

def2-SVP Basis Set

The benchmarking results obtained using the def2-SVP basis set are close to those obtained using the 6-31G(d) basis set.

Table S3. Benchmarking results using def2-SVP basis set in kcal/mol.

	A	***B***	***TS2***	***TS3***	***TS4***	*MAE*
APFD	0.00	-2.64	3.11	0.20	8.18	3.24
B1B95	0.00	-3.50	3.75	-0.43	9.32	4.05
B1LYP	0.00	2.26	1.25	3.62	3.87	1.09
B3LYP	0.00	1.09	1.19	2.66	4.39	1.51
B3PW91	0.00	-2.62	2.77	0.09	7.76	3.07
B97-D3	0.00	-0.94	-0.19	1.59	3.89	2.76
BH&HLYP	0.00	5.39	2.84	6.55	3.98	1.56
BLYP	0.00	-0.11	-0.31	1.30	3.38	2.78
BMK	0.00	3.18	2.24	1.63	6.60	1.08
CAM-B3LYP	0.00	2.46	3.03	4.20	5.53	0.28
B3LYP-D3(BJ)	0.00	1.79	0.58	3.43	3.70	1.47
BLYP-D3(BJ)	0.00	0.75	-1.06	2.24	2.55	2.72
CAM-B3LYP-D3(BJ)	0.00	2.84	2.74	4.59	5.14	0.23
PBE0-D3(BJ)	0.00	-2.88	3.23	0.18	8.48	3.41
PBE-D3(BJ)	0.00	-5.12	1.64	-2.00	7.90	4.48
HSEH1PBE	0.00	-3.00	3.34	-0.03	8.46	3.51
LC-ωHPBE	0.00	-0.54	6.92	2.79	10.44	3.58
M06	0.00	-3.72	4.88	0.27	8.85	4.10
M06-2X	0.00	-1.52	5.04	1.25	8.78	3.33
M06-L	0.00	-6.45	4.59	-2.03	9.67	5.49
M11	0.00	-0.91	5.88	1.28	9.76	3.62
MN12-L	0.00	-2.03	1.97	0.96	6.58	2.56
MN12-SX	0.00	-1.12	2.77	1.31	6.95	2.19
MN15	0.00	-0.31	3.32	2.15	7.99	2.17
N12-SX	0.00	-4.08	3.71	-0.91	9.15	4.27
O3LYP	0.00	-4.05	2.76	-0.94	7.87	3.71
PBE0	0.00	-3.27	3.54	-0.23	8.86	3.78
PBE	0.00	-5.53	1.99	-2.44	8.30	4.71
PBEh1PBE	0.00	-2.99	3.48	0.01	8.57	3.56
PW6B95-D3	0.00	-1.87	2.98	0.77	7.85	2.79
SOGGA11X	0.00	0.38	4.03	2.86	7.13	1.78
TPSS	0.00	-4.22	2.02	-1.43	7.76	3.98
TPSSh	0.00	-3.44	2.64	-0.64	8.04	3.51
X3LYP	0.00	1.21	1.30	2.79	4.48	1.40
mPW1PW91	0.00	-2.47	3.23	0.31	8.20	3.20
revTPSS	0.00	-5.20	2.48	-2.19	9.01	4.62
τ-HCTH hyb.	0.00	-0.64	1.35	0.83	5.93	2.23
ωB97X	0.00	1.40	5.26	3.99	7.35	1.61
ωB97X-D	0.00	0.92	3.51	2.94	6.61	1.37

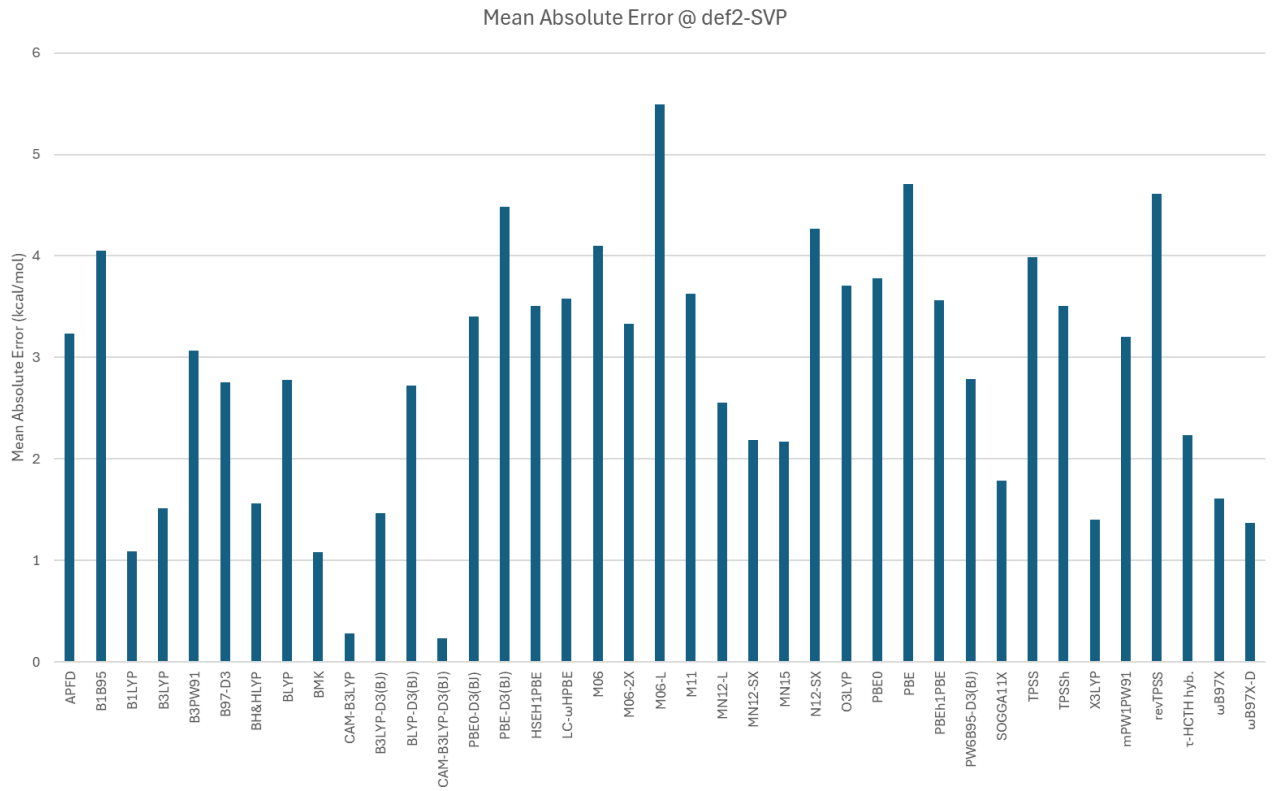

Figure S3. Mean absolute error (MAE) values for benchmarking functionals using the def2-SVP basis set, relative to the CCSD(T)/CBS reference energies in kcal/mol. The CAM-B3LYP-D3(BJ) and CAM-B3LYP exhibits outstanding accuracy for the barbaralyl cation system.

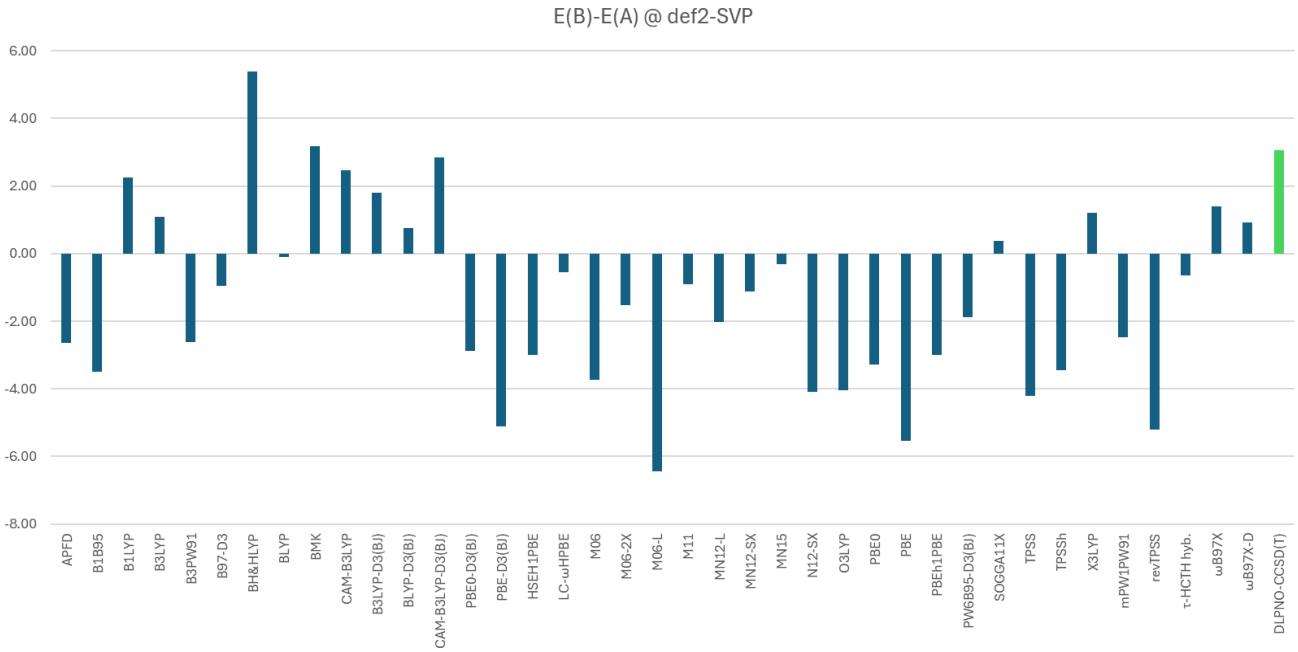

Figure S4. Relative energy of **B** (kcal/mol) for benchmarking functionals using the def2-SVP basis set, relative to the CCSD(T)/CBS reference energies in kcal/mol. The reference result is highlighted in green.

Therefore, we identified that for small split-valance basis sets, CAM-B3LYP appears to offer the best match to the DLPNO-CCSD(T)/CBS results in this region of the PES.

Electronic Energies

Table S4. Single point energy under CCSD(T)/CBS level of theory in hartree.

	A	***B***	***TS2***	***TS3***	***TS4***
DLPNO-CCSD(T)	-347.5225019	-347.5176235	-347.5182562	-347.5157533	-347.5138757

6-31G(d) basis set

Table S5. Benchmarking result using 6-31G(d) basis set in hartree.

	A	***B***	***TS2***	***TS3***	***TS4***
APFD	-347.7413371	-347.7443928	-347.7369334	-347.740398	-347.7286902
B1B95	-347.8663042	-347.8705896	-347.860941	-347.8662741	-347.8519278
B1LYP	-347.8246185	-347.8198434	-347.8231643	-347.8181878	-347.8189061
B3LYP	-348.0243565	-348.0214771	-348.0229979	-348.0194604	-348.0178402
B3PW91	-347.8989521	-347.9020049	-347.8951003	-347.8982052	-347.8869819
B97-D3	-347.7976411	-347.7980346	-347.7985154	-347.7945093	-347.7918902
BH&HLYP	-347.8054095	-347.795536	-347.8014669	-347.7942787	-347.7995164
BLYP	-347.8533535	-347.8524615	-347.8543727	-347.8506574	-347.8484558
BMK	-347.7790378	-347.7749019	-347.7750195	-347.776565	-347.7679027
CAM-B3LYP	-347.8142017	-347.8091386	-347.8099748	-347.806898	-347.8058809
B3LYP-D3(BJ)	-348.0605155	-348.0565094	-348.0601268	-348.0543953	-348.0550951
BLYP-D3(BJ)	-347.8976867	-347.8954272	-347.8998924	-347.8935012	-347.8941146
CAM-B3LYP-D3(BJ)	-347.8306212	-347.8249455	-347.8268524	-347.822685	-347.8229206
PBE0-D3(BJ)	-347.6318794	-347.6353028	-347.62728	-347.6309613	-347.6187494
PBE-D3(BJ)	-347.5920566	-347.599133	-347.5899614	-347.594634	-347.5798701
HSEH1PBE	-347.6415827	-347.6452147	-347.6367942	-347.6409962	-347.6284935
LC-ωHPBE	-347.7765743	-347.7763507	-347.7662117	-347.7716082	-347.7603975
M06	-347.75434	-347.7596159	-347.7471188	-347.7535484	-347.7405419
M06-2X	-347.8690374	-347.870288	-347.8616083	-347.8664647	-347.8554038
M06-L	-347.9784143	-347.9883514	-347.9714443	-347.9814817	-347.9630545
M11	-347.7968673	-347.798014	-347.788056	-347.7948714	-347.7813923
MN12-L	-347.6896846	-347.6911834	-347.6872624	-347.6871031	-347.6798683
MN12-SX	-347.7343793	-347.7343218	-347.7307512	-347.7312506	-347.7240636
MN15	-347.5929549	-347.5923234	-347.5881583	-347.5889052	-347.5807124
N12-SX	-347.87623	-347.8814935	-347.8708802	-347.8770106	-347.8620795
O3LYP	-347.9073783	-347.91252	-347.9035061	-347.9081285	-347.8953044
PBE0	-347.6135975	-347.617642	-347.6085061	-347.6133346	-347.5998521
PBE	-347.5709731	-347.5787058	-347.5683267	-347.574259	-347.5581474
PBEh1PBE	-347.6499437	-347.6535658	-347.6449395	-347.6493017	-347.6366688
PW6B95-D3	-348.5017695	-348.5034492	-348.4976284	-348.4998127	-348.4897349
SOGGA11X	-347.9400006	-347.9383352	-347.9341575	-347.9349269	-347.9288781
TPSS	-348.0993515	-348.1049373	-348.0967132	-348.1010031	-348.0873902
TPSSh	-348.064271	-348.068593	-348.0606463	-348.0646631	-348.0518541
X3LYP	-347.8505704	-347.8474803	-347.8490308	-347.8454704	-347.8439024
mPW1PW91	-347.951083	-347.953888	-347.9465032	-347.9499815	-347.9383917
revTPSS	-348.0121652	-348.0192995	-348.0088121	-348.0150242	-347.9982284

τ-HCTH hyb.	-347.9721002	-347.9722144	-347.9703461	-347.9702192	-347.9629586
ωB97X	-347.9346998	-347.931514	-347.9269102	-347.9279807	-347.9232769
ωB97X-D	-347.9124072	-347.909892	-347.9074111	-347.9073578	-347.9021697

def2-SVP basis set

Table S6. Benchmarking result using def2-SVP basis set in hartree

	A	***B***	***TS2***	***TS3***	***TS4***
APFD	-347.4893292	-347.4935329	-347.4843747	-347.4890095	-347.4762919
B1B95	-347.6105772	-347.6161556	-347.6046009	-347.6112564	-347.5957244
B1LYP	-347.5685617	-347.5649534	-347.566564	-347.5627903	-347.5623871
B3LYP	-347.7692122	-347.7674806	-347.7673166	-347.7649662	-347.7622242
B3PW91	-347.6470852	-347.6512563	-347.6426768	-347.6469385	-347.6347113
B97-D3	-347.5509665	-347.5524695	-347.5512746	-347.5484262	-347.5447656
BH&HLYP	-347.5488846	-347.5402881	-347.5443551	-347.5384536	-347.5425374
BLYP	-347.5969069	-347.5970812	-347.5974079	-347.5948281	-347.5915197
BMK	-347.5068277	-347.5017537	-347.50326	-347.5042266	-347.4963095
CAM-B3LYP	-347.5595539	-347.5556361	-347.5547305	-347.5528662	-347.5507404
B3LYP-D3(BJ)	-347.8053712	-347.8025129	-347.8044455	-347.7999011	-347.7994791
BLYP-D3(BJ)	-347.6412402	-347.6400469	-347.6429277	-347.6376719	-347.6371785
CAM-B3LYP-D3(BJ)	-347.5759734	-347.5714431	-347.5716082	-347.5686532	-347.56778
PBE0-D3(BJ)	-347.3797521	-347.3843438	-347.3746067	-347.3794665	-347.3662414
PBE-D3(BJ)	-347.3403942	-347.3485508	-347.3377813	-347.3435736	-347.3278063
HSEH1PBE	-347.3888668	-347.3936465	-347.3835405	-347.3889081	-347.3753893
LC-ωHPBE	-347.5275083	-347.5283671	-347.5164857	-347.5230561	-347.5108679
M06	-347.4922947	-347.4982306	-347.4845246	-347.4918588	-347.4781954
M06-2X	-347.6093698	-347.6117945	-347.6013302	-347.6073751	-347.5953774
M06-L	-347.7293678	-347.7396493	-347.722049	-347.7326066	-347.7139578
M11	-347.5279944	-347.5294487	-347.5186238	-347.5259555	-347.512436
MN12-L	-347.4121884	-347.4154274	-347.4090549	-347.4106512	-347.4016976
MN12-SX	-347.4292088	-347.4309982	-347.424791	-347.4271219	-347.4181326
MN15	-347.2846199	-347.2851143	-347.2793306	-347.2811874	-347.2718815
N12-SX	-347.6304824	-347.6369884	-347.6245686	-347.6319248	-347.615905
O3LYP	-347.6584177	-347.6648647	-347.6540131	-347.6599149	-347.6458839
PBE0	-347.3614703	-347.366683	-347.3558328	-347.3618398	-347.3473442
PBE	-347.3193108	-347.3281236	-347.3161465	-347.3231986	-347.3060835
PBEh1PBE	-347.3973604	-347.402123	-347.3918117	-347.3973399	-347.3836983
PW6B95-D3	-348.2442256	-348.2472094	-348.2394715	-348.2429929	-348.2317166
SOGGA11X	-347.6806761	-347.680078	-347.6742616	-347.6761111	-347.6693123
TPSS	-347.8519119	-347.858632	-347.8486987	-347.8541866	-347.8395465
TPSSh	-347.8158806	-347.8213703	-347.8116703	-347.8169076	-347.8030613
X3LYP	-347.5953482	-347.5934201	-347.5932732	-347.5909083	-347.5882111
mPW1PW91	-347.6986754	-347.702619	-347.6935329	-347.698179	-347.6856094
revTPSS	-347.7599169	-347.7682047	-347.7559668	-347.763401	-347.7455655
τ-HCTH hyb.	-347.7199868	-347.7210141	-347.7178316	-347.7186621	-347.7105361
ωB97X	-347.6806915	-347.6784534	-347.6723089	-347.6743317	-347.6689821
ωB97X-D	-347.6592548	-347.657795	-347.6536535	-347.6545757	-347.6487182

Divergent Results for Geometry Optimization on Barbaralyl Rearrangement

However, as our preliminary study utilizing the Minnesota M06-2X exchange-correlation functional failed to optimize **TS2**, it is also important to benchmark the behavior of the functionals regarding if they can optimize to correct structures and have correct local curvature about each stationary points. Here Y refers to optimization to stationary point of correct nature, **N** means optimization did not converge or clearly converged to another stationary point and TS/MIN means they optimized to a TS or minimum while it should be a minimum or a TS.

We discovered that a lot of functionals lead to incorrect characterization of **TS2** as a minimum or failed to optimize to a structure alike **TS2**. In particular, we realize that range-separated hybrids or (to a lesser degree) functionals with moderate amount of exact exchange seems to have better success at predicting correct nature of the stationary points as well as locating all key structures.

6-31G(d) basis set

Table S7. Summary of the identification of stationary points using different density functionals with the 6-31G(d) basis set. "Y" indicates that the structure was correctly identified as the expected minimum or transition state, while "**N**" indicates that the optimization converged to a different structure. "MIN" denotes that TS was optimized to a minimum instead of a saddle point. "TS" denotes that it was optimized to a saddle point instead of a minimum.

	A	***B***	***TS2***	***TS3***	***TS4***
APFD	Y	Y	Y	Y	Y
B1B95	Y	Y	**N**	Y	Y
B1LYP	Y	Y	MIN	Y	Y
B3LYP	Y	Y	MIN	Y	Y
B3PW91	Y	Y	Y	Y	Y
B97-D3	Y	Y	MIN	Y	Y
BH&HLYP	Y	Y	MIN	Y	Y
BLYP	Y	Y	MIN	Y	Y
BMK	TS	Y	MIN	Y	Y
CAM-B3LYP	Y	Y	Y	Y	Y
B3LYP-D3(BJ)	Y	Y	MIN	Y	Y
BLYP-D3(BJ)	Y	Y	MIN	Y	Y
CAM-B3LYP-D3(BJ)	Y	Y	Y	Y	Y
PBE0-D3(BJ)	Y	Y	Y	Y	Y
PBE-D3(BJ)	Y	Y	**N**	Y	Y
HSEH1PBE	Y	Y	**N**	Y	Y
LC-ωHPBE	Y	Y	**N**	Y	Y
M06	Y	Y	Y	Y	Y
M06-2X	Y	Y	**N**	Y	Y
M06-L	Y	Y	**N**	Y	Y
M11	Y	Y	**N**	Y	Y
MN12-L	Y	Y	MIN	Y	Y
MN12-SX	Y	Y	Y	Y	Y
MN15	Y	Y	Y	Y	Y
N12-SX	Y	Y	**N**	Y	Y

O3LYP	Y	Y	**N**	Y	Y
PBE0	Y	Y	**N**	Y	Y
PBE	**N**	Y	**N**	**N**	Y
PBEh1PBE	Y	Y	**N**	Y	Y
PW6B95-D3(BJ)	Y	Y	Y	Y	Y
SOGGA11X	Y	Y	Y	Y	Y
TPSS	Y	Y	**N**	Y	Y
TPSSh	Y	Y	**N**	Y	Y
X3LYP	Y	Y	MIN	Y	Y
mPW1PW91	Y	Y	**N**	Y	Y
revTPSS	**N**	Y	**N**	**N**	Y
τ-HCTH hyb.	Y	Y	Y	Y	Y
ωB97X	Y	Y	Y	Y	Y
ωB97X-D	Y	Y	Y	Y	Y

def2-SVP basis set

Table S8. Summary of the identification of stationary points using different density functionals with the def2-SVP basis set. "Y" indicates that the structure was correctly identified as the expected minimum or transition state, while "**N**" indicates that the optimization converged to a different structure. "MIN" denotes that TS was optimized to a minimum instead of a saddle point. "TS" denotes that it was optimized to a saddle point instead of a minimum. "2nd order " denotes that it was optimized to a secondary order saddle point.

	A	***B***	***TS2***	***TS3***	***TS4***
APFD	Y	Y	**N**	Y	Y
B1B95	Y	Y	**N**	Y	Y
B1LYP	Y	Y	MIN	Y	Y
B3LYP	Y	Y	MIN	Y	Y
B3PW91	Y	Y	N	Y	Y
B97-D3	Y	Y	MIN	Y	Y
BH&HLYP	Y	Y	MIN	Y	Y
BLYP	Y	Y	MIN	Y	Y
BMK	TS	2nd order	MIN	Y	Y
CAM-B3LYP	Y	Y	Y	Y	Y
B3LYP-D3(BJ)	Y	Y	MIN	Y	Y
BLYP-D3(BJ)	Y	Y	MIN	Y	Y
CAM-B3LYP-D3(BJ)	Y	Y	Y	Y	Y
PBE0-D3(BJ)	Y	Y	**N**	Y	Y
PBE-D3(BJ)	Y	Y	**N**	Y	Y
HSEH1PBE	Y	Y	**N**	Y	Y
LC-ωHPBE	Y	Y	**N**	Y	Y
M06	Y	Y	**Y**	Y	Y
M06-2X	Y	Y	**N**	Y	Y
M06-L	Y	Y	**N**	Y	Y
M11	Y	Y	**N**	Y	Y
MN12-L	Y	Y	Y	Y	Y
MN12-SX	Y	Y	Y	Y	Y
MN15	Y	Y	Y	Y	Y

N12-SX	Y	Y	**N**	Y	Y
O3LYP	Y	Y	**N**	Y	Y
PBE0	Y	Y	**N**	Y	Y
PBE	**N**	Y	**N**	**N**	Y
PBEh1PBE	Y	Y	**N**	Y	Y
PW6B95-D3(BJ)	Y	Y	Y	Y	Y
SOGGA11X	Y	Y	Y	Y	Y
TPSS	Y	Y	**N**	Y	Y
TPSSh	Y	Y	**N**	Y	Y
X3LYP	Y	Y	Y	Y	Y
mPW1PW91	Y	Y	**N**	Y	Y
revTPSS	**N**	Y	**N**	**N**	Y
τ-HCTH hyb.	Y	Y	Y	Y	Y
ωB97X	Y	Y	Y	Y	Y
ωB97X-D	Y	Y	Y	Y	Y

Data table for results in the main text

Table S9. Summary of energies reported in the main text (in hartree). The Gibbs free energy corrections were calculated at a temperature of 138.15 K.

Structure	E_{low}	E_{high}	ΔG	G_{final}
H2O	-76.380248	-76.376776	0.015602	-76.361174
1	-424.210660	-423.905855	0.171221	-423.734634
TS1(A)	-424.207839	-423.903682	0.167439	-423.736243
INT	-424.208718	-423.908958	0.164953	-423.744005
TS1(B)	-424.208677	-423.909692	0.164860	-423.744832
A	-347.814457	-347.522668	0.142879	-347.379789
B	-347.809410	-347.517999	0.142345	-347.375654
TS2	-347.810360	-347.518496	0.142424	-347.376072
TS3	-347.807163	-347.515902	0.141843	-347.374059
TS4	-347.806113	-347.514094	0.142329	-347.371765
C	-347.833755	-347.540694	0.143573	-347.397121
D	-347.851919	-347.553519	0.141709	-347.411810
E	-347.898392	-347.595350	0.143548	-347.451802
F	-347.808883	-347.512973	0.141780	-347.371193
G	-347.870718	-347.570478	0.143297	-347.427181
H	-347.850514	-347.548435	0.139019	-347.409416
TS5	-347.797953	-347.504697	0.142792	-347.361905
TS6	-347.783148	-347.495166	0.143189	-347.351977
TS7	-347.801359	-347.509501	0.138823	-347.370678
TS8	-347.824995	-347.530777	0.138186	-347.392591
TS9	-347.800526	-347.507859	0.139089	-347.368770
TS10	-347.849347	-347.550299	0.139074	-347.411225
TS11	-347.842428	-347.548763	0.139721	-347.409042
TS12	-347.799731	-347.506888	0.138177	-347.368711
BC8H9	-334.841725	-334.702053	0.139672	-334.416900
TS_{BC8H9}	-334.818266	-334.680038	0.138228	-334.397598

[4.3.0] Shapeshifting Rearrange Mechanism

CAM-B3LYP

As mentioned in the manuscript, when the barbaralyl cation undergoes ring opening to form the [4.3.0] non-classical carbocation, the potential energy surfaces calculated using the DLPNO-CCSD(T)/CBS and CAM-B3LYP/6-31G(d) level show some discrepancies regarding the existence of certain stationary points, particularly secondary carbocations, as true minima. At the CAM-B3LYP/6-31G(d) level of theory, a minimum (**H**) and a nearby transition structure (**TS10**) were optimized, suggesting a stepwise, two-step 1,2-H shift mechanism for the conversion of structure **D** to structure **E**. However, when single-point energy corrections were performed at the higher DLPNO-CCSD(T)/CBS level, the electronic energy of **H** was found to be higher than that of **TS10**, indicating that the stepwise mechanism is actually asynchronously concerted. Instead, the higher-level calculations suggest that the transformation from **D** to **E** proceeds *via* a 1,3-H shift mechanism, with a relatively flat potential energy surface following the first proton shift. For IRCs, please refer to the IRC section in the end of the SI.

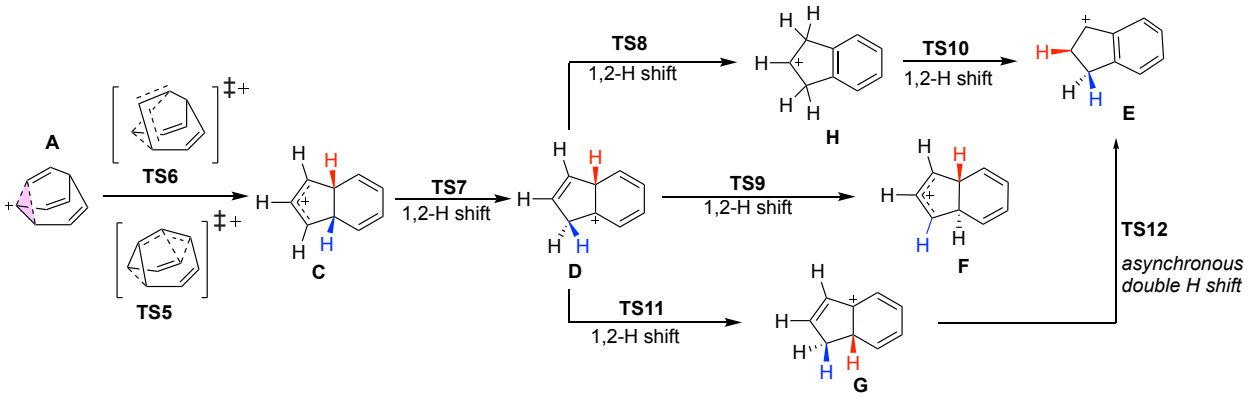

Figure S5. The mechanism predicted at CAM-B3LYP/6-31G(d) level of theory. **H** has a lower energy than **TS8** and **TS10** under this level, confirmed by IRC. While under higher DLPNO-CCSD(T)/CBS level, **H** is higher than **TS10**.

M06-2X

At this ring opening stage, the M06-2X gives better description of the energy profile, which does describe the process that **D** to **E** conversion as a 1,3 shift. As the structure **H** does not corresponds to a minimum anymore, **D** is capable of isomerizing to **E** *via* **TS8** directly. Moreover, under M06-2X functional, the structure of **H** turns to be a distinct double hydride shift transition state **TS13** where the two sequential shifts occur in a highly asynchronous manner to generate **E'**.

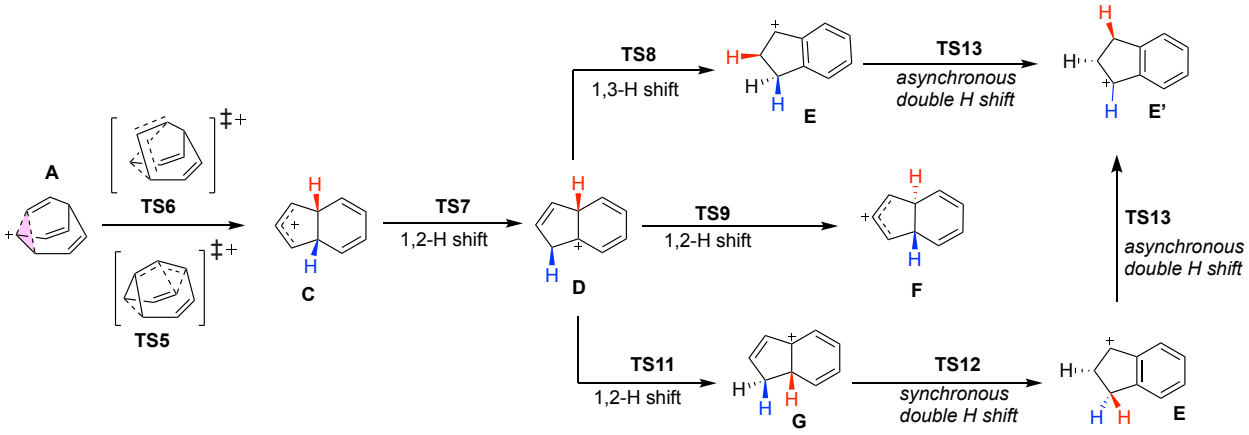

Figure S6. The mechanism predicted at M06-2X/6-31G(d) level of theory. The structure of **H** in Figure S5 turns to be the transition structure **TS13** that connects **E** and **E'.**

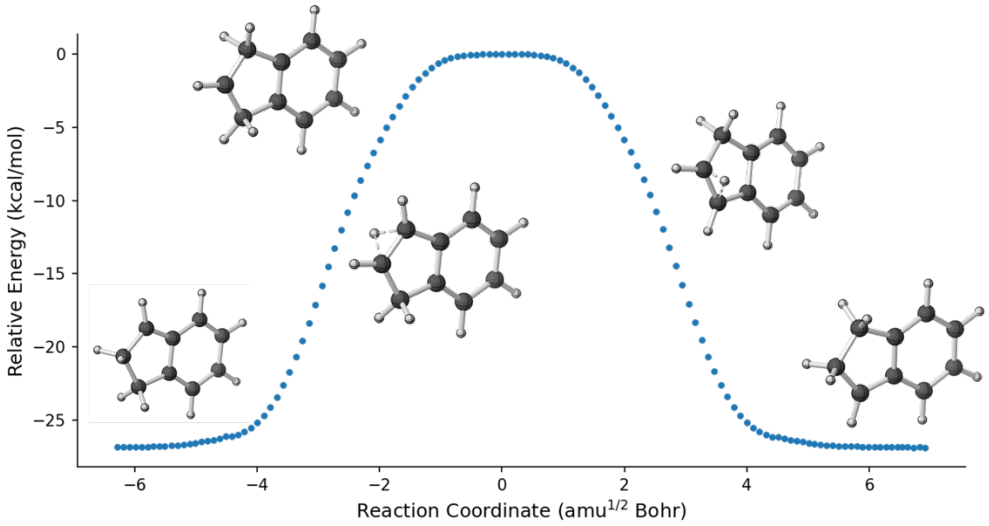

Figure S7. The intrinsic reaction coordinate of **TS13**, a double hydride shift that interconverts **E** and **E'**.

NMR

For the structure that are optimized under CAM-B3LYP/6-31G(d) and M06-2X/6-31G(d) level of theory, we conducted the NMR calculation based on the same methodology: 1. NMR calculation under revTPSS/pcSseg-1 level of theory. 2. taking TMS as the reference for chemical shifts. The comparison between the two levels is summarized below:

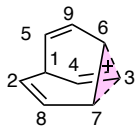

A

Table S10. computational NMR result of **A**

		^{13}C shift		
C center	isotropic value (CAM-B3LYP structure)	^{13}C shift (CAM-B3LYP structure)	isotropic value (M06-2X structure)	^{13}C shift (M06-2X structure)
4	-33.506	**221.7**	-29.257	**218.2**
8,9	69.309	**118.9**	70.942	**118.0**
1	122.708	**65.5**	123.227	**65.7**
2,5	57.22	**131.0**	59.418	**129.5**
3	101.918	**86.3**	103.41	**85.5**
6,7	86.115	**102.1**	88.007	**100.9**
TMS(C)	188.215	**0**	188.043	**0**
		^{1}H shift		
C center	isotropic value (CAM-B3LYP structure)	^{1}H shift (CAM-B3LYP structure)	isotropic value (M06-2X structure)	^{1}H shift (M06-2X structure)
4	21.886	**9.99**	22.117	**9.88**
8,9	25.486	**6.39**	25.613	**6.39**
1	25.827	**6.05**	25.891	**6.11**
2,5	25.401	**6.48**	25.518	**6.48**
3	26.74	**5.14**	26.893	**5.11**
6,7	25.316	**6.56**	25.396	**6.60**
TMS(H)	31.88	**0**	32.00	**0**

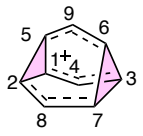

B

Table S11. computational NMR result of **B**

^{13}C shift

C center	isotropic value (CAM-B3LYP structure)	^{13}C shift (CAM-B3LYP structure)	isotropic value (M06-2X structure)	^{13}C shift (M06-2X structure)
4,8,9	56.882	**132.8**	55.454	**132.1**
1,2,3,5,6,7	112.287	**76.8**	111.395	**118.0**
TMS(C)	188.215	**0**	188.043	**0**

^{1}H shift

C center	isotropic value (CAM-B3LYP structure)	^{1}H shift (CAM-B3LYP structure)	isotropic value (M06-2X structure)	^{1}H shift (M06-2X structure)
4,8,9	25.381	**6.50**	25.502	**6.50**
1,2,3,5,6,7	25.919	**5.96**	26.035	**5.97**
TMS(H)	31.88	**0**	32.00	**0**

Potential Energy Surface

Besides the CAM-B3LYP functional, we also constructed the potential energy surface in terms of C2-C5 and C3-C6 distances and its 2D projection using the ωB97X-D and M06-2X functionals. The difference between these three levels of theory is mainly the relative energy of **B** with respect to **A**. Since the M06-2X functional predicts a lower energy for **B**, the downhill pathway from **TS4** directly connects it to **B** instead of **TS2** (**TS2** is no longer a saddle point on the surface). The relative potential energy of **B** and the PESs are depicted below:

Table S12. Comparison of energetics for the barbaralyl cation and related structures calculated using different levels of theory.

	M06-2X/6-31G(d)	ωB97X-D/6-31G(d)	CAM-B3LYP/6-31G(d)
B relative to **A** (kcal/mol)	-0.7	1.6	3.2
TS2 located?	No	Yes	Yes

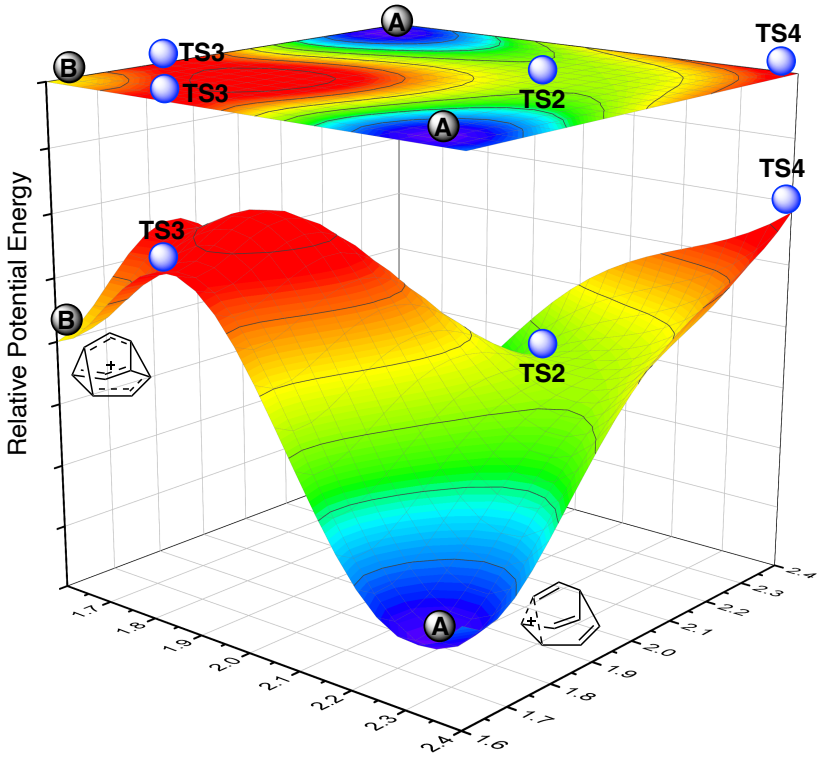

Figure S8. PES under CAM-B3LYP/6-31G(d) level of theory with critical structures labeled.

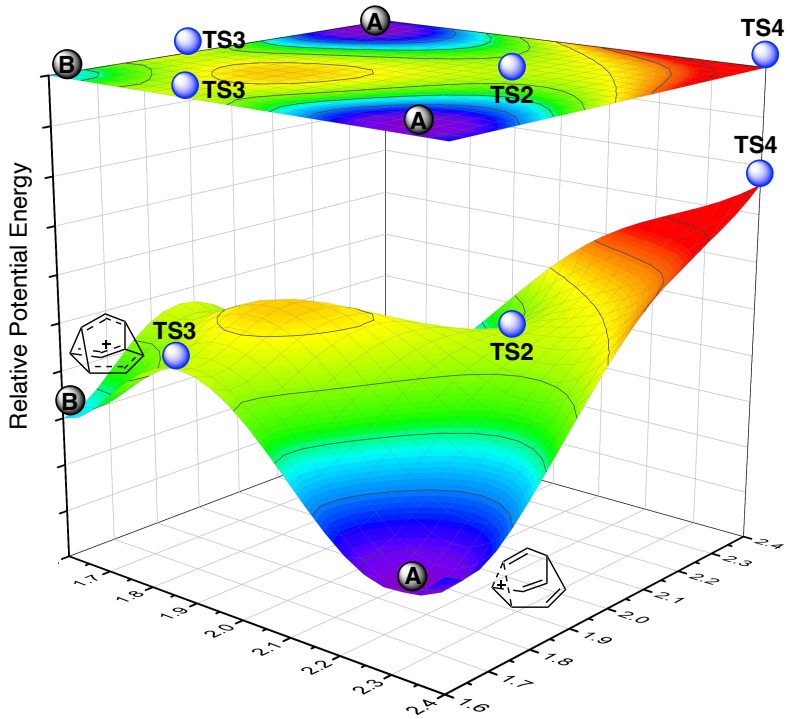

Figure S9. PES under ωB97X-D/6-31G(d) level of theory with critical structures labeled.

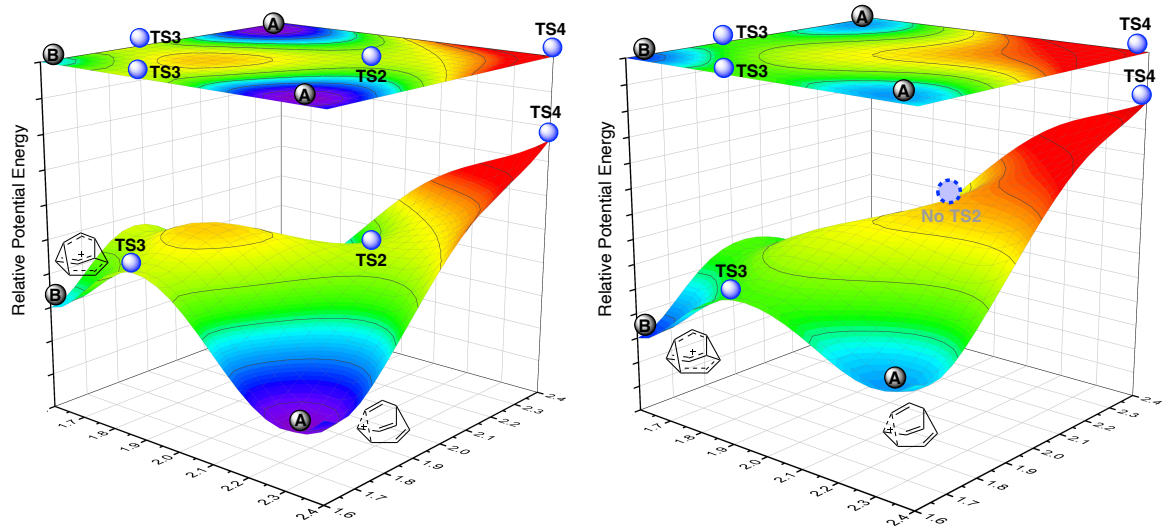

Figure S10. PES at M06-2X/6-31G(d) level of theory with critical structures labeled.

Metadynamics

Free energy surface

The well-tempered metadynamics simulation was carried out using ORCA 5.0.4 using CAM-B3LYP/6-31G(d) level of theory at 138.15K with the canonical sampling velocity rescaling thermostat and propagated for 17600 fs where it appears to be reasonably converged. The slight deviation from ideal symmetry of the free energy profile is due to stochastic nature of the MD simulation and the path through the phase space.

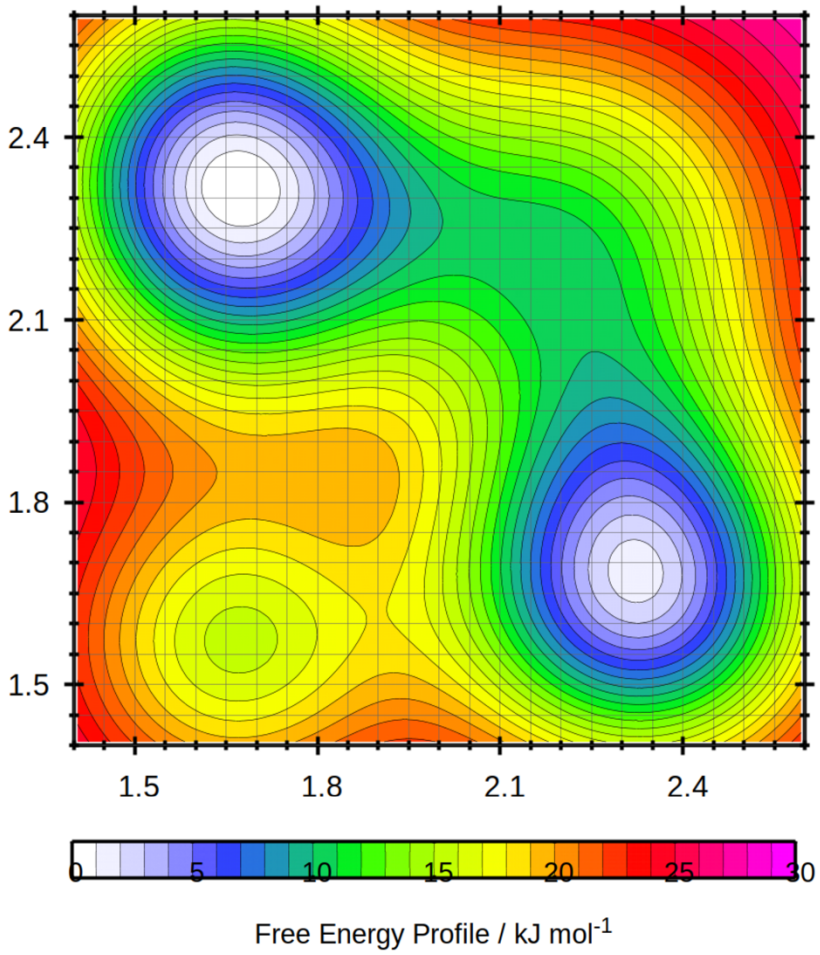

Figure S11. Free energy surface of the barbaralyl cation system constructed using metadynamics simulations. The FES is plotted based on the same geometric parameters as PES.

Input file

```
! CAM-B3LYP 6-31G(d) def2/J RIJCOSX MD
%pal nproc 16 end
%maxcore 7000
%md
Timestep 1.0_fs
Initvel 138.15_K
Thermostat CSVR 138.15_K Timecon 50.0_fs
Dump Position Stride 1 Filename "trajectory.xyz"
Manage_Colvar Define 1 Distance Atom 10 Atom 14
Manage_Colvar Define 2 Distance Atom 1 Atom 2
Metadynamics Colvar 1 Scale 1.0_A Wall Upper 2.6 50.0 Range 1.4 2.6 100
Metadynamics Colvar 2 Scale 1.0_A Wall Upper 2.6 50.0 Range 1.4 2.6 100
Metadynamics HillSpawn 30 0.3 0.2 Store 200
Metadynamics WellTempered 2500_K
constraint add center 0..17
restart
Run 100000
end
*xyz 1 1
 C          0.03669936   -1.29786178    0.75877000
 C          0.03669936   -1.29786178   -0.75877000
 C         -1.31124764   -0.78925278   -0.00000000
 H         -0.09508364   -2.27031678    1.21936300
 H         -0.09508364   -2.27031678   -1.21936300
 H         -2.13304764   -1.49396478   -0.00000000
 C         -1.50991964    0.57111822   -0.00000000
 H         -2.50987864    0.99070622   -0.00000000
 C         -0.36815364    1.43049922   -0.00000000
 H         -0.53899464    2.50207022   -0.00000000
 C          0.78451536    0.98140522    0.92320000
 H          1.41824136    1.77067722    1.30784200
 C          0.76804636   -0.28679178    1.43280000
 H          1.33209236   -0.53470078    2.32467100
 C          0.78451536    0.98140522   -0.92320000
 H          1.41824136    1.77067722   -1.30784200
 C          0.76804636   -0.28679178   -1.43280000
 H          1.33209236   -0.53470078   -2.32467100
*
```

AIMD details

Ab initio molecular dynamics (AIMD) simulations were performed using the Progdyn package to investigate both downhill and uphill reaction pathways. The simulations employed the Gaussian 16 C.01 version for quantum chemistry calculations at the CAM-B3LYP/6-31G(d) level of theory at 138.15K. Three types of simulations were conducted: classical downhill dynamics without zero-point energy sampling, quasi-classical downhill dynamics with zero-point energy sampling, and quasi-classical uphill dynamics. The classical downhill simulations provide insight into the potential energy surface, while the quasi-classical simulations incorporate the effects of zero-point energy, enabling a more accurate description of the reaction dynamics.

Uphill MD simulation

The uphill molecular dynamics (MD) simulation involves defining the potential at the initial sampling, which corresponds to the direction of breaking the C2-C5 bond, facilitating the conversion from structure **B** to **A1**. The trajectories are terminated at 1 ps (1000 steps, with each 1 femtosecond step). Throughout the entire trajectory, the encountered minima are stored based on the following criteria:

Table S13. bond length definition (Angstrom) for structure capture during uphill MD simulation

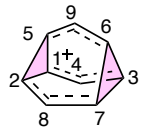

B

CRITICAL BONDS	C2-C5, C3-C6, C1-C2, C6-C7, C4-C5, C3-C3	
B	all bonds < 1.60	
A1	C2-C5 > 2.40	other bonds < 1.70
A2	C3-C6 > 2.40	
A3	C1-C2 > 2.40	
A4	C6-C7 > 2.40	
A5	C4-C5 > 2.40	
A6	C3-C7 > 2.40	

To evaluate the uphill MD simulation, we applied energy inputs of 3 kcal/mol and 10 kcal/mol to test the effect on the C2-C5 bond stretching. The results indicate that higher energy input increases the formation ratio of A1. This is because the increased momentum drives the molecule towards the formation that aligns with the input energy. As illustrated in Figures S12 and S13, an input of 3 kcal/mol results in 31% formation of A, whereas 10 kcal/mol results in 64% formation of A as the first minimum encountered after escaping from B.

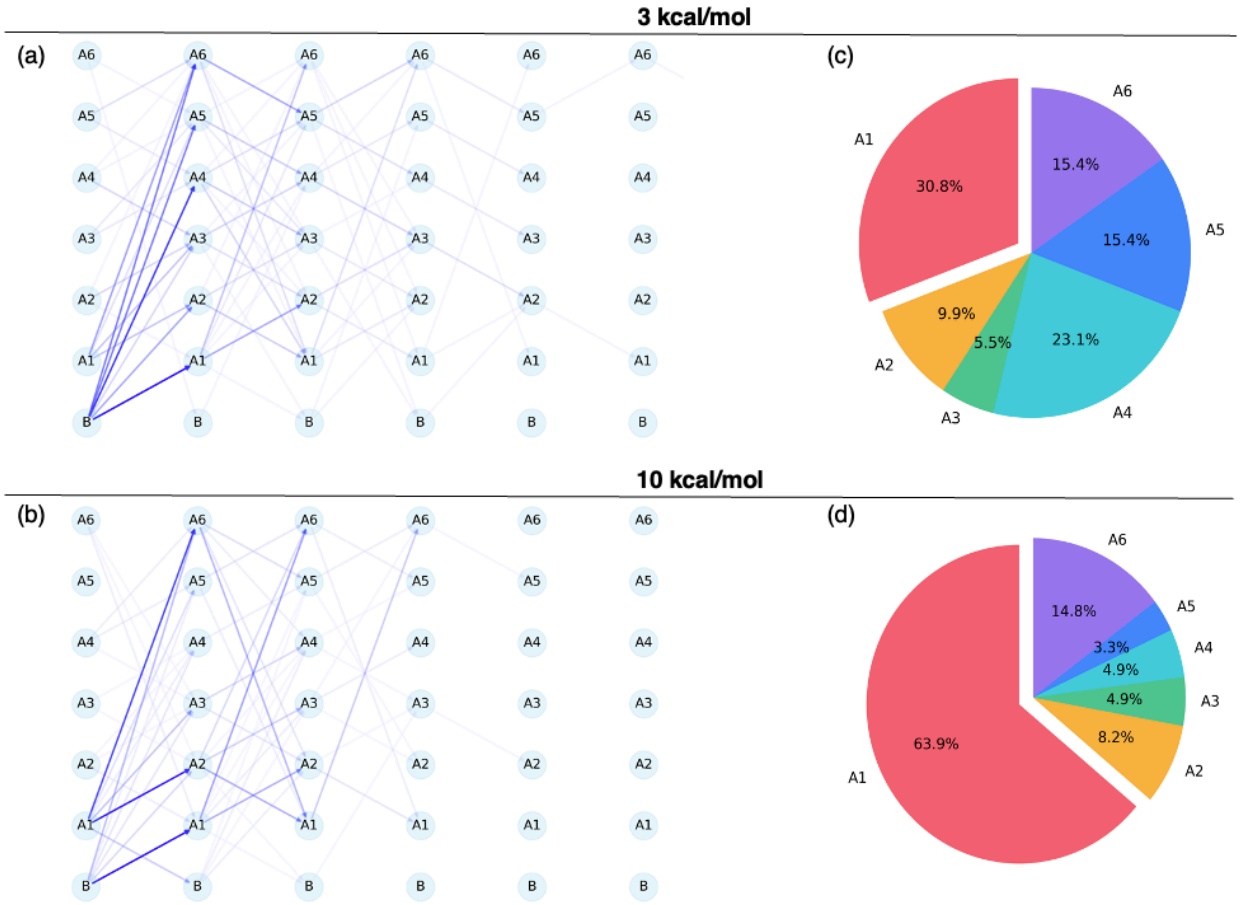

Figure S12. Left: Network visualization depicting minima encountered in uphill simulations from B towards A1. Sequential nodes from left to right denote successive minima encountered along each trajectory with (a) 3 kcal/mol and (b) 10 kcal/mol excess energy. The thick-ness of lines reflects the relative population for different types of pathways, with denser populations of trajectories indicated by greater thickness. Right: Distribution of the first minimum encountered for uphill simulations with (c) 3 kcal/mol and (d) 10 kcal/mol excess energy.

A total of 188 trajectories were collected for a deposit energy of 10 kcal/mol, capturing 468 minima interconversions. The scatter plot below illustrates the results for each trajectory, with the first structure encountered represented by red, followed by orange, yellow, green, blue, and purple, adhering to the order of the rainbow colors. The trajectories are arranged from left to right, with their IDs ranging from 1 to 188. This visualization provides a clear overview of the sequence of structures encountered along each trajectory. The result agrees with the tree-shaped and pie plot in the manuscript, showing that most of the trajectories lead to **A1** as the very first product. Though some of them bounce back to **B**, even with extra energy, the following product is more likely to be **A1**. However, as the energy decreases to 3 kcal/mol (the potential barrier is 1 kcal/mol), the preference to form **A1** diminishes, as shown in the main text and figures below. A total of 174 trajectories were collected for a deposit energy of 3 kcal/mol, capturing 441 minima interconversions. The same scatter plot is shown below.

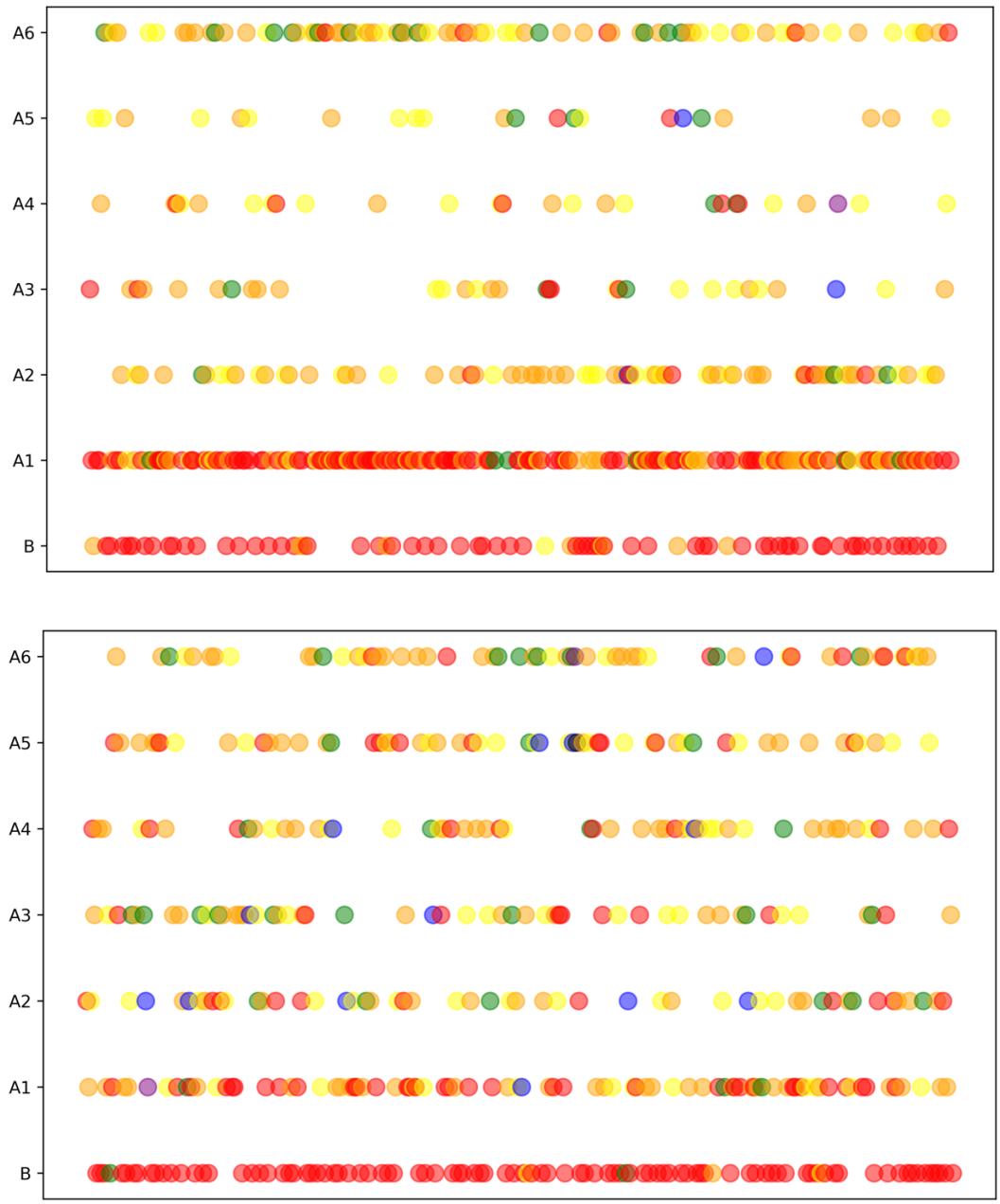

Figure S13. Scatter plot visualizing the minima encountered during each trajectory of the uphill AIMD simulation with a deposit energy of 10 kcal/mol (top) and 3 kcal/mol (bottom).

Downhill MD Simulation

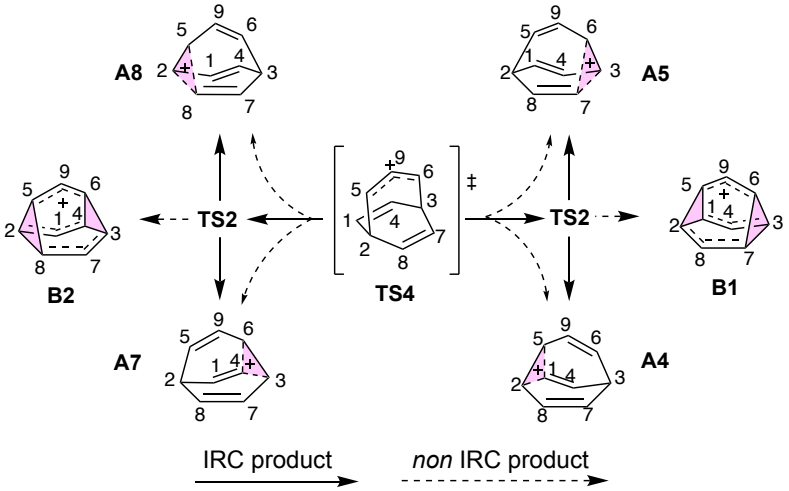

Scheme S1. Illustration of the six minima connected by TS4 with 2D structures by ChemDraw.

Each trajectory in the downhill AIMD simulations was set to have a maximum duration of 500 femtoseconds. However, if the geometry of the system meets the predefined stopping criteria, the trajectory is terminated immediately. The stopping criteria are summarized as follows:

CRITICAL BONDS	**C1-C5, C5-C8, C6-C7, C4-C6**	
B1	C1-C5, C6-C7< 1.60	
B2	C5-C8, C4-C6 < 1.60	
A5	C1-C5 > 2.40	C6-C7 < 1.65
A4	C6-C7 > 2.40	C1-C5 < 1.65
A7	C5-C8 > 2.40	C4-C6 < 1.65
A8	C4-C6 > 2.40	C5-C8 < 1.65

Table S14. Stopping criteria of downhill AIMD simulation

In total, 638 classical AIMD trajectories and 536 quasi-classical AIMD trajectories were generated. The number of trajectories in each group is labeled in main text figure 10.

Trifurcation under M06-2X/6-31G(d)

The unique potential energy surface topology obtained using the M06-2X functional reveals a natural trifurcation surface, which not only leads to the formation of three distinct products but also features three symmetry-related exit channels at one side. Due to the symmetry around **TS4**, the surface naturally connects six minima without encountering any additional transition states along the pathway.

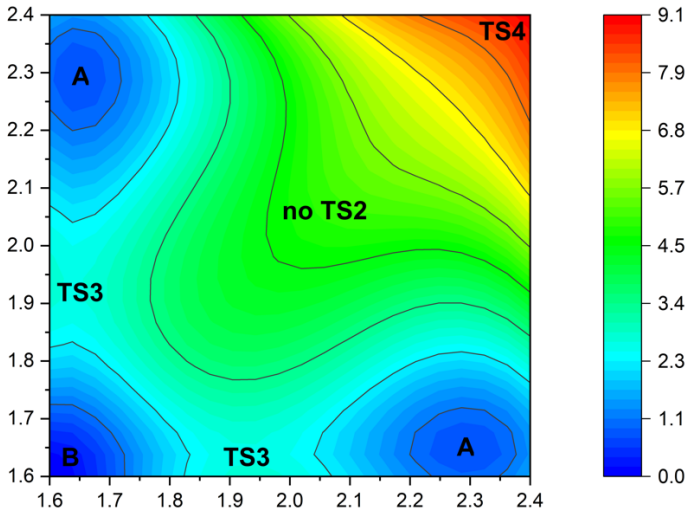

Figure S14. 2D potential energy surface calculated at the M06-2X/6-31G(d) level of theory. The steepest descent path (minimum energy pathway) from **TS4** leads directly to product **B** without encountering any stationary points. Simultaneously, the two equivalent **A** structures can be accessed *via* symmetric downhill path from **TS4**.

The downhill AIMD simulation reveals its complexity. In our quasi-classical downhill MD simulations initiated from **TS4**, we also uncovered pathways that directly connect various forms of **A** and **B**. Similarly to what we reported in the main text, **TS4** not only connects state **B1** to its mirrored **B2**, but also provides a direct route to **A4, A5, A7** and **A8** states on either side of the **B** states. Projections onto the CV1, CV2, and CV3 planes (same CV as figure 9 in the manuscript), clearly show six distinct minima corresponding to **B1**, **B2**, and the associated **A4, A5, A7** and **A8** being accessed. The emergence of **A**s is 'direct' from **TS4**, as the trajectories circumvent the **B1** and **B2** minima instead of traversing them. Only 133 trajectories are collected while with out of the 17 distinct trajectory types identified, 43% depict a transition from one side of **B** to an opposing side of **A** (purple bins). Meanwhile, 11% connect two minima on the same side (pink bins), and only 32% bridge **B1** to **B2** (blue bins), aligning with results obtained from IRC analysis.

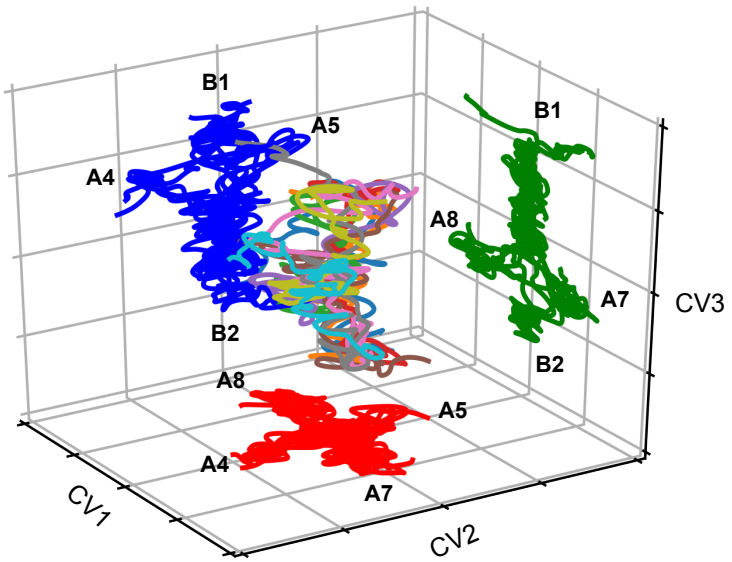

Figure S15. The trajectories are visualized with respect to the coordinates CV1, CV2, and CV3. CV1 is defined by R(C5,C8) – R(C4,C6); CV2 is defined by R(C6,C7) – R(C1,C5); and for CV3, (R(C5,C8) + R(C4,C6)) – (R(C6,C7) + R(C1,C5)). To better capture the six products, projections on each plane are distinctly colored in red, blue, and green.

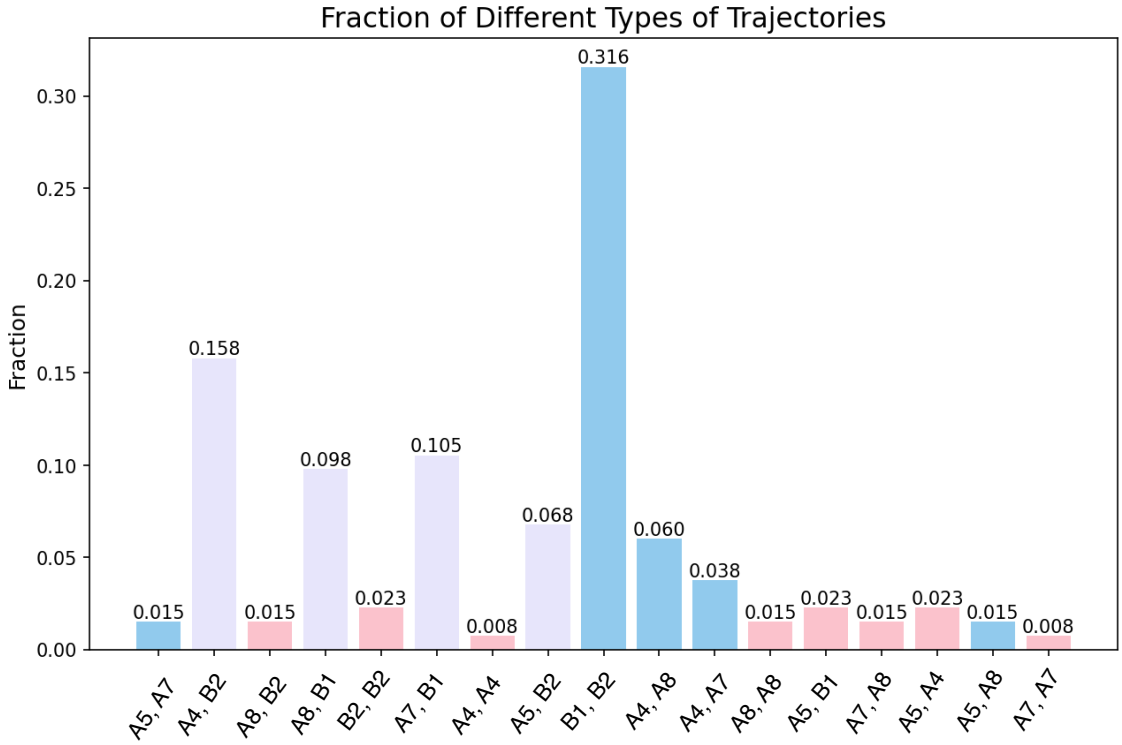

Figure S16. The proportion of trajectories collected from downhill AIMD simulations that were initiated from **TS3**. Trajectories that connect minima from the left and right sides are depicted in blue and purple: those connecting **B** to **A** are in purple, while the rest are in blue. Trajectories in red indicate 'recrossing' events, where connections occur between two minima on the same side.

progdyn.conf file

The progdyn.conf file is shown below. The `classical` parameter is set to `0` for quasi-classical AIMD simulations and `1` for classical AIMD simulations. Uphill dynamics is defined by enabling the cannonball option with the energy specified as either 3 or 10 kcal/mol. The `etolerance` parameter is set to 999 for uphill dynamics, which means that there is no checking on the energy of the sampled structures. For downhill sampling, the `etolerance` is set to 0.3 kcal/mol. The `reversetraj` is turned on as "true" for downhill MD simulation but turned off as "false"for uphill. Temperature was set to be 138.15K.

```
#This is the configuration file for PROGDYN.  This file is read by progdynstarterHP and
# the awk programs proggenHP, prog1stpoint, prog2ndpoint, and progdynb.
#The programs won't read anything past the first blank line,
#and this file must end with a blank line.
#The program has a number of default values but they are unlikely to be what you want.
#Do not delete lines - rather, comment out lines for unwanted options.
#The values here are read repeatedly and most can be changed in the middle of running jobs
#***The keywords are case sensitive.  The following keywords should always be defined:***
#***method, charge, multiplicity, memory, processors, title
#*** method --The following word is copied exactly to the gaussian input file.
method CAM-B3LYP/6-31g(d)
#To do a nonstandard route, make nonstandard 1.  For normal calcs, use nonstandard 0 or else
leave it out.
#Then make a file called "nonstandard" containing the nonstandard route with no extra lines.
#nonstandard 0
# NMRoptions NMRtype 1 will add a section for an NMR calc at every NMRevery intervals.
The NMRmethod is the calculation used
#for the NMR calculation.  The awk program progNMRm might be useful as a starting point for
pulling out the data from files named
#NMRlist
#NMRtype 1
#NMRmethod ub3lyp/genecp
#NMRevery 4
#Use geometry linear to get the program to recognize 3N-5 normal modes instead of 3N-6 when
reading from freqinHP
#geometry linear
#Rotationmode controls whether molecular rotations are turned on. They should be turned on
with rotationmode 1 but this can be set
#at 0 to reproduce older calculations.
#rotationmode 1
#*** method2 --The options here are restricted, unrestricted, and read. restricted is the default
#If the method is U..., put unrestricted here and the .com files will have in them guess=mix.
#If you put read here, the .com files will contain guess=tcheck, which sometimes makes things
faster, sometimes not.
#The use of read requires a specifically defined checkpoint file name using the keyword
checkpoint.
method2 restricted
```

```
charge 1
multiplicity 1
processors 16
#*** memory --The following "word" is copied exactly to the gaussian input file after %mem=.
memory 32GB
#*** killcheck and checkpoint -- You can use a specifically defined checkpoint file name by putting
#the name after the keyword checkpoint.  This is necessary if you use the read option with method2.
#Defined checkpoint names are an unnecessary modest hastle and if you do not want to bother, use killcheck 1
killcheck 1
#checkpoint g09.chk
#*** diagnostics -- 0 prints out nothing extra, 1 (default) prints out extra stuff to a
#file "diagnostics", 2 adds more stuff, 3 adds velocities to a file "vellist"
#4 adds the apparent temperature to vellist, but this is meaningless with quasiclassical calculations
diagnostics 2
#*** title -- the title keyword must be followed by exactly four words
title Rh t21 cis test
#*** initialdis -- 0 (default) turns off displacement of the normal modes, so that all trajectories start from the same place
# and only the energies and signs of the motion in the modes are randomized
# 1 gives a flat distribution of displacements where all of the possible values are equally likely
# 2 (recommended) gives a QM-like gaussian distribution of displacements, so that displacements in the middle are more likely that
# those at the end by 1/e
initialdis 2
#*** timestep -- this is the time between points in the trajectory.  Typical values would be 1E-15 or 0.5E-15 or 0.25E-15
timestep 1E-15
#*** scaling -- this lets you scale the gaussian frequencies by a constant
scaling 1.0
temperature 138.15
#*** method3, method4, method5, and method6 -- These keywords let you add extra lines to the gaussian input file.
#method3 and method4 add lines at the top of the input after the lines defining the method, and
#this is useful to implement things like the iop for mPW1k
#method5 and method6 add lines after the geometry, after a blank line of course
#only a single term with no spaces can be added, one per method line.  Here are some examples to uncomment if needed
#method3 empiricaldispersion=gd3
#method3 scrf=(pcm,Solvent=water)
#add the line below with big structures to get it to put out the distance matrix and the input orientation
method4 iop(2/9=2000)
```

#method4 scrf=(pcm,solvent=dmso,read)
#method4 IOp(3/76=1000001970)IOp(3/77=0800008000)IOp(3/78=0700010000)
#method5 radii=bondi
#method6
#*** methodfile -- This keyword lets you add more complicated endings to gaussian input files
#such as a gen basis set. Put after the keyword the number of lines in a file you create called
#methodfile that contains the test you want to add to the end of the gaussian input
methodfile 0
#*** numimag --This tells the program the number of imaginary frequencies in the starting structure.
#if 0, treats as ground state and direction of all modes is random
#if 1, motion along the reaction coordinate will start out in the direction defined by searchdir
#if 2, only lowest freq will go direction of searchdir and other imag mode will go in random direction
numimag 1
#*** searchdir -- This keyword says what direction to follow the mode associated with the imaginary frequency.
#The choices are "negative" and "positive". Positive moves in the direction defined in the gaussian frequency calculation
#for the imaginary frequency, while negative moves in the opposite direction. The correct choice can be made either
#by a careful inspection of the normal modes and standard orientation geometry, or by trial and error.
searchdir negative
#*** classical -- for quassiclassical dynamics, the default, use 0. for classical dynamics, use 1
#if there are no normal modes and the velocities are to be generated from scratch, use classical 2
classical 0
#*** DRP, saddlepoint, and maxAtomMove --to run a DRP use 'DRP 1' in the line below, otherwise leave it at 0 or comment it out
#the treatment of starting saddlepoints is not yet implemented so use saddlepoint no
#if DRP shows oscillations then decrease maxAtomMove
#DRP 1
#saddlepoint no
#maxAtomMove 0.01
#*** cannonball -- The program can "fire" a trajectory from a starting position toward a particular target, such as toward
#a ts. To use this, make a file cannontraj with numAtom lines and three numbers per line that defines the vector
#for firing the trajectory, relative to the starting geometry's standard orientation. The number following cannonball sets
#the extra energy being put into the structure in kcal/mol
cannonball 10
#*** keepevery --This tells the program how often to write the gaussian output file to file dyn, after the first two points.
#Use 1 for most dynamics to start with, but use a higher number to save on disk space or molden loading time.

keepevery 1
#*** highlevel --For ONIOM jobs, the following line states the number of highlevel atoms, #which must come before the medium level atoms. Use some high value such as 999 if not using ONIOM
highlevel 999
#linkatoms 1
#*** fixedatom1, fixedatom2, fixedatom3, and fixedatom4 - These fix atoms in space.
#Fixing one atom serves no useful purpose and messes things up, while fixing two atoms #fixes one distance and fixing three has the effect of fixing three distances, not just two
#in current form fixed atoms only are meant to work with no displacements, that is, initialdis=0
#fixedatom1 2
#fixedatom2 3
#fixedatom3 19
#*** boxon and boxsize - With boxon 1, a cubic box is set such that atoms that reach the edge #are reflected back toward the middle. Useful for dynamics with solvent molecules. This is a crude
#implementation that is ok for a few thousand femtoseconds but will not conserve energy long term.
#Set the box size so as to fit the entire initial molecule but not have too much extra room.
#The dimensions of the box are two times the boxsize, e.g. boxsize 7.5 leads to a box that is 15 x 15 x 15 angstroms
boxon 0
boxsize 7.5
#*** displacements -- This keyword lets you set the initialdis of particular modes by using a series of lines of the format
displacements NumberOfMode InitialDisForThatMode, as in the example below. You should be able to do as many of these as you like
you might consider this for rotations where a straight-line displacement goes wrong at large displacements
The choices for InitialDisForThatMode are 0, 1, 2, and 10, where 10 does the same thing as 0 but is maintained for now because
a previous version of the program had a bug that made 0 not work.
#*** etolerance --This sets the allowable difference between the desired energy in a trajectory and the actual
#energy, known after point 1 from the potential energy + the kinetic energy in the initial velocities.
#The unit is kcal/mol and 1 is a normal value for mid-sized organic systems. For very large and floppy molecules, a larger value
#may be needed, but the value must stay way below the average thermal energy in the molecule (not counting zpe).
#If initialdis is not 0 and few trajectories are being rejected, decrease the value.
etolerance 999
#*** controlphase --It is sometimes useful to set the phase of particular modes in the initialization of trajectories.
#The format is controlphase numberOfModeToControl positive or controlphase numberOfModeToControl negative.

#controlphase 3 positive
#*** damping -- The damping keyword lets you add or subtract energy from the system at each point, by multiplying the velocities
#by the damping factor. A damping of 1 has no effect, and since you mostly want to change the energy slowly, normal values range
#from 0.95 to 1.05. The use of damping lets one do simulated annealing - you add energy until the structure is moving enough
#to sample the kinds of possibilities you are interested in, then you take away the energy slowly.
damping 1
#*** reversetraj --This keyword sets the trajectories so that both directions from a transition state are explored.
reversetraj false
#updated Aug 9, 2007 to include the possibility of classical dynamics by the keyword classical
#updated Jan 2008 to include fixed atoms, ONIOM jobs, keepevery, and box size
#update Feb 2008 to include methodfile parameter
updated Nov 2008 to allow for start without an initial freq calc using classical = 2
update Aug 2010 to include etolerance, damping controlphase and reversetraj

Tunneling Effect

The tunneling effect was investigated using the Polyrate/Gaussrate packages at the CAM-B3LYP/6-31G(d) level of theory under different temperatures. Both the small-curvature tunneling (SCT) and zero-curvature tunneling (ZCT) approximations were employed, and the contribution of tunneling to the overall reaction rate was determined based on the kappa factor.

The kappa factor, also known as the "tunneling correction" or "transmission coefficient" in transition state theory, is calculated as the ratio of the Boltzmann average of the quantum transmission probability to the Boltzmann average of the classical transmission probability, with the threshold energy set at the peak of the adiabatic ground-state energy. The fraction of the reaction rate attributable to tunneling is given by:

$$\frac{quantum\ transmission\ probability}{quantum\ transimission\ probility\ +\ classical\ transimission\ probility} = \frac{\kappa\ -1}{\kappa}$$

Results

Table S15. The overall tunneling effects computed under CAM-B3LYP/6-31G(d) level of theory. In the manuscript, only results at 138.15, 188.15 and 273.15 K are displayed.

	T(K)	κ_{ZCT}	κ_{SCT}	fraction of rate due to tunneling (ZCT)	fraction of rate due to tunneling (SCT)
	123.15	1.1157	1.6055	10.37%	37.71%
	138.15	1.0810	1.3385	7.49%	25.29%
	158.15	1.0564	1.1963	5.34%	16.41%
TS2	188.15	1.0372	1.1121	3.59%	10.08%
	238.15	1.0221	1.0598	2.16%	5.64%
	273.15	1.0165	1.0431	1.62%	4.13%
	298.15	1.0137	1.0353	1.35%	3.41%
	123.15	2.0486	2.2137	51.19%	54.83%
	138.15	1.7608	1.8718	43.21%	46.58%
	158.15	1.5352	1.6078	34.86%	37.80%
TS3	188.15	1.3508	1.3951	25.97%	28.32%
	238.15	1.2049	1.2291	17.01%	18.64%
	273.15	1.1518	1.1692	13.18%	14.47%
	298.15	1.1257	1.1400	11.17%	12.28%
	123.15	1.4126	1.6300	29.21%	38.65%
	138.15	1.2840	1.3892	22.12%	28.02%
	158.15	1.1978	1.2539	16.51%	20.25%
TS4	188.15	1.1310	1.1617	11.58%	13.92%
	238.15	1.0780	1.0941	7.24%	8.60%
	273.15	1.0583	1.0699	5.51%	6.53%
	298.15	1.0485	1.0580	4.63%	5.48%

Input files of Polyrate/Gaussrate

The relevant sections from the input file, namely the PATH, TUNNEL, and RATE sections, are provided below for reference.

```
*PATH

 SCALEMASS  1.00
 INTMU   3
 SSTEP   0.005
 INH     9

 SRANGE
 SLP 1.00
 SLM -1.00
 END

 RPM       pagem

 SIGN    product

 IDIRECT  1

 COORD CART

 RODS
 PRPATH
 COORD    1 11
 INTERVAL 1
 XMOL

 END

*TUNNEL
 ZCT
 SCT
 SCTOPT
  lagrange 4
END

*RATE
   TST
   CVT
   CUS 2
   BOTHK

   SIGMAF 1
```

```
  PRDELG ON


TEMP
  123.15
  138.15
  158.15
  188.15
  238.15
  273.15
  298.15
END
```

Kinetics of total scrambling w/ tunneling

Table S16. Half-life time of total scrambling under -150°C and -135°C.

T(°C)	w/o tunneling	κ_{SCT}	w/ tunneling (SCT)	κ_{ZCT}	w/ tunneling (SCT)
$t_{1/2}$ at -150°C (computed)	200 μs	1.6300	124 μs	1.4126	143 μs
$t_{1/2}$ at -135°C (computed)	20 μs	1.3892	14 μs	1.284	15 μs

At -150°C, the half-life of total scrambling (corresponding to **TS4**, with an energy barrier of 5.0 kcal/mol) decreased from 200 μs to approximately 140 μs, equivalent to a reduction in the effective barrier to 4.9 kcal/mol. Dynamic NMR measurements reveal that the observed 6:3 ratio of partial scrambling corresponds to a total scrambling barrier of approximately 5.0 kcal/mol. Since the tunneling effect only lowers the effective barrier by 0.1 kcal/mol, our conclusion remains unchanged: even accounting for tunneling, NMR spectroscopy is still capable of resolving the split signal.

Solvolysis of 1

Scheme 1 in the main text illustrates the solvolysis of compound **1** to generate the barbaralyl cation **2**. The transition state **TS1(A)** is highly asynchronous, initially dissociating to a structure resembling **TS2** (labeled as **INT**), followed by a very shallow C-C bond breaking transition state **TS1B** leading to the complex of A···H_2O on the intrinsic reaction coordinate. However, single-point electronic energy correction reveals that **TS1(B)** has a lower electronic energy compared to **INT**, indicating that this solvolysis is indeed concerted but highly asynchronous on the *ab initio* potential energy surface (PES) corrected using the DLPNO-CCSD(T)/CBS method.

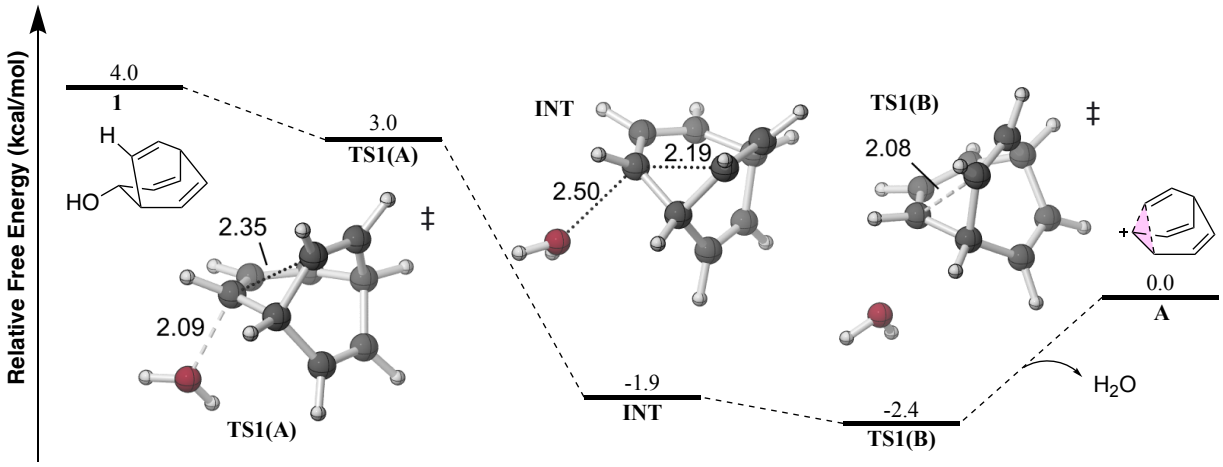

Figure S17. Energy profile of solvolysis of **1** at DLPNO-CCSD(T)/CBS//CAM-B3LYP/6-31G(d) level of theory at 138.15 K with 3D structures visualized by *CYLview1.0*.

Localized Orbital Analysis of B

The Adaptive Natural Density Partitioning (AdNDP) analysis[46] was carried out using Multiwfn 3.8(dev)[47] using Kohn-Sham wavefunction at CAM-B3LYP/6-31G(d) level of theory.
We first searched for two centered orbitals, their occupation number (Nocc) and degeneracy were listed below and plotted using isovalue of 0.05:

Isosurface	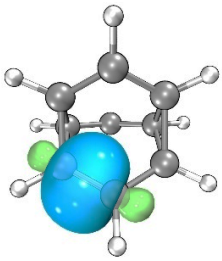	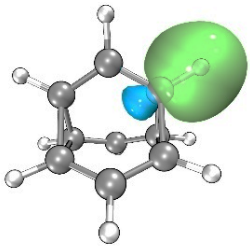	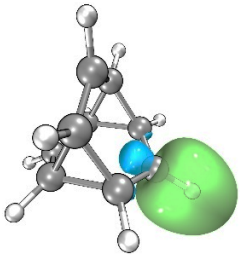	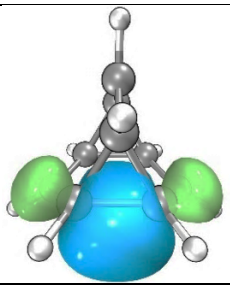
Nocc	1.985	1.975	1.964	1.795
Degeneracy	6	6	3	6
Type	σ_{C-C}	σ_{C-H}	σ_{C-H}	σ_{C-C}

And lastly one remaining delocalized orbital from searching with all centers / 9 carbon centers corresponding to mostly interaction of three p orbitals

Isosurface	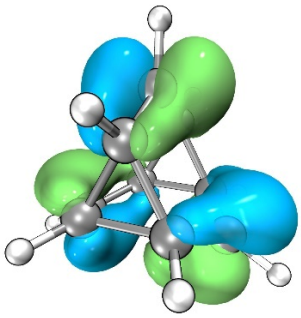
Nocc	2.000
Degeneracy	1
Type	Carbon p orbitals

2-Norbornyl and A

The bond length comparison under CAM-B3LYP/6-31G(d) level of theory between compound A and 2-norbornyl (both have a 3-center 2- electron delocalization geometry) is displayed below:

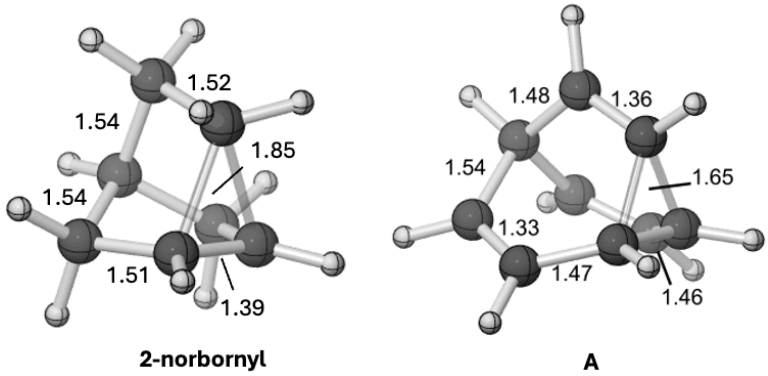

Figure S18. The geometry of 2-norbornyl and **A** visualized by *CYLView 1.0* with critical bond lengths labeled in angstrom.

The barbaralyl cation **A** exhibits somewhat different electron delocalization than the 2-norbornyl cation, with its the 3-center/2-electron bonding array also interacting with the adjacent methine groups.

BC_8H_9

The only transition structure we were able to locate resembling any of the transition structures for BC_8H_9 was a [3s,3s] sigmatropic shift. The TS and its IRC are depicted below.

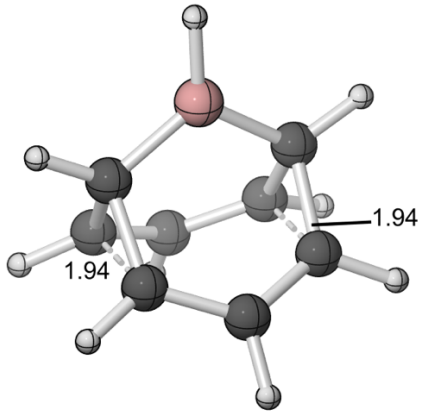

Figure S19. The Cope rearrangement TS (BC_8H_9) visualized by *CYLView 1.0* with critical bond lengths labeled in angstrom.

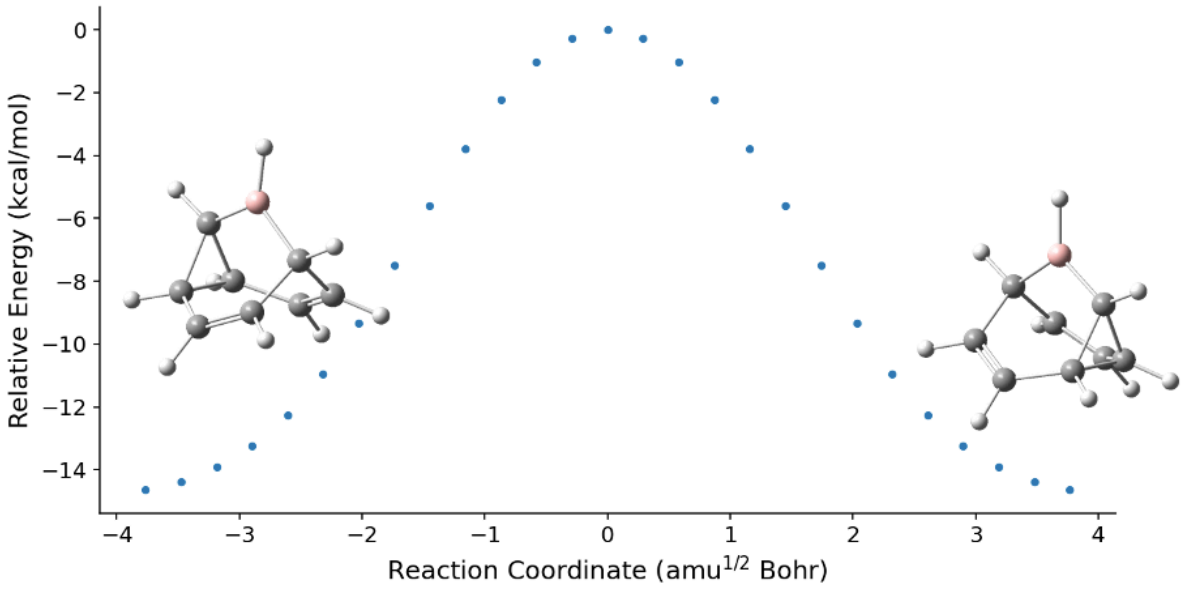

Figure S20. The intrinsic reaction coordinate of the Cope rearrangement TS (BC_8H_9).

Intrinsic Reaction Coordinates

Intrinsic Reaction Coordinate (IRC) plots for the transition state structures, displaying the energy profile along the reaction path. The 3D structures of the minima connected by each transition state are shown above and below the respective IRC plot. The energy axis represents the relative energy in kcal/mol with respect to the TS energy, which is set to zero.

TS1(A)

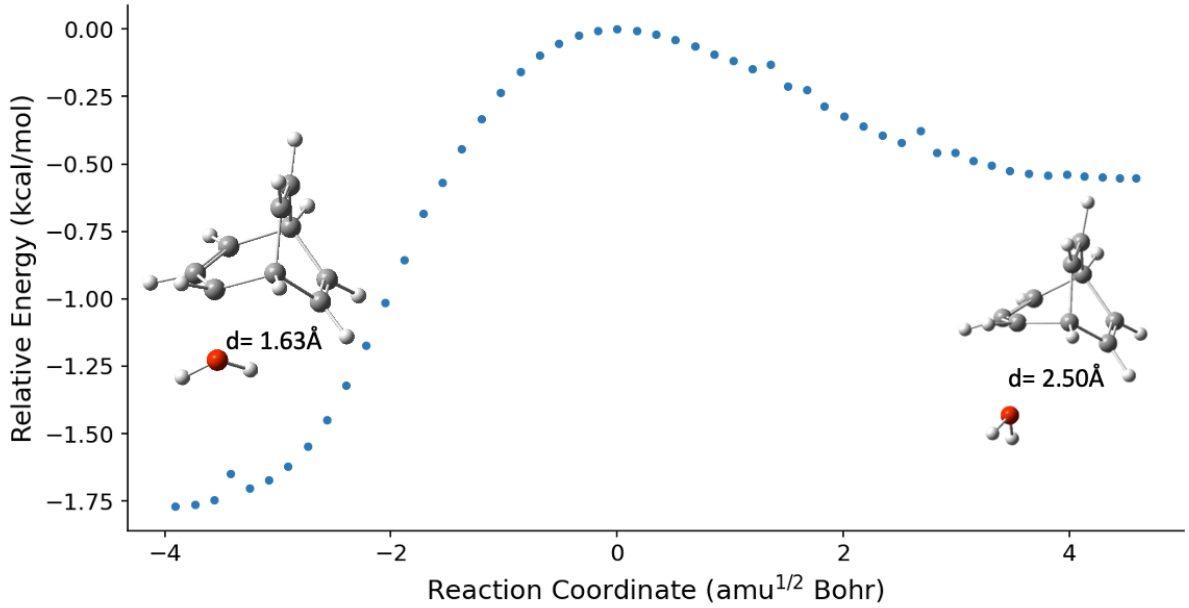

TS1(B)

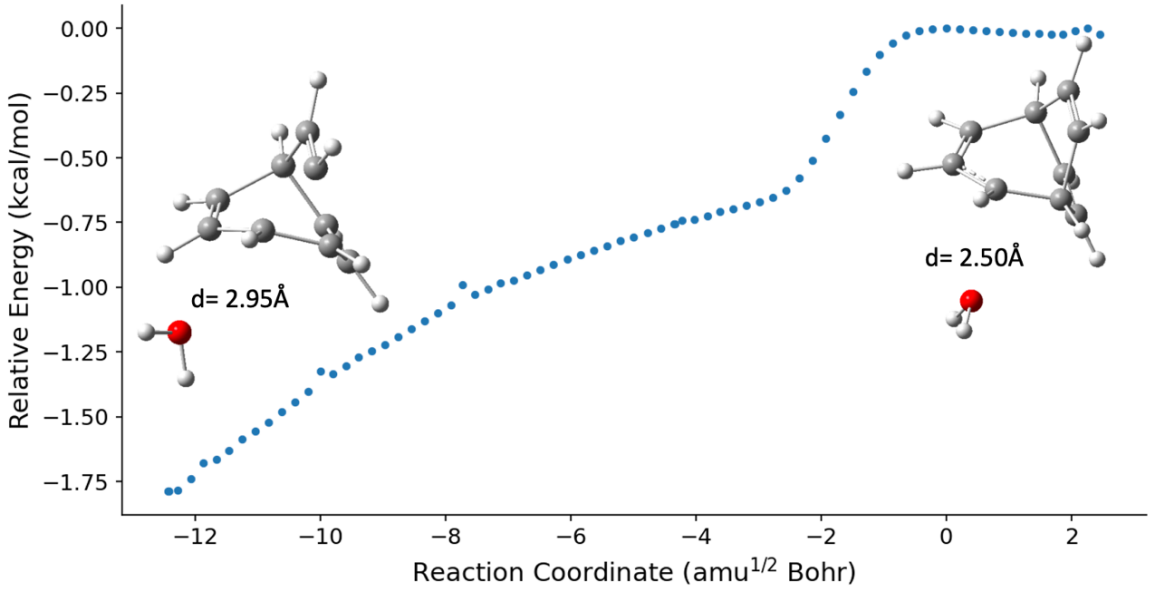

TS2

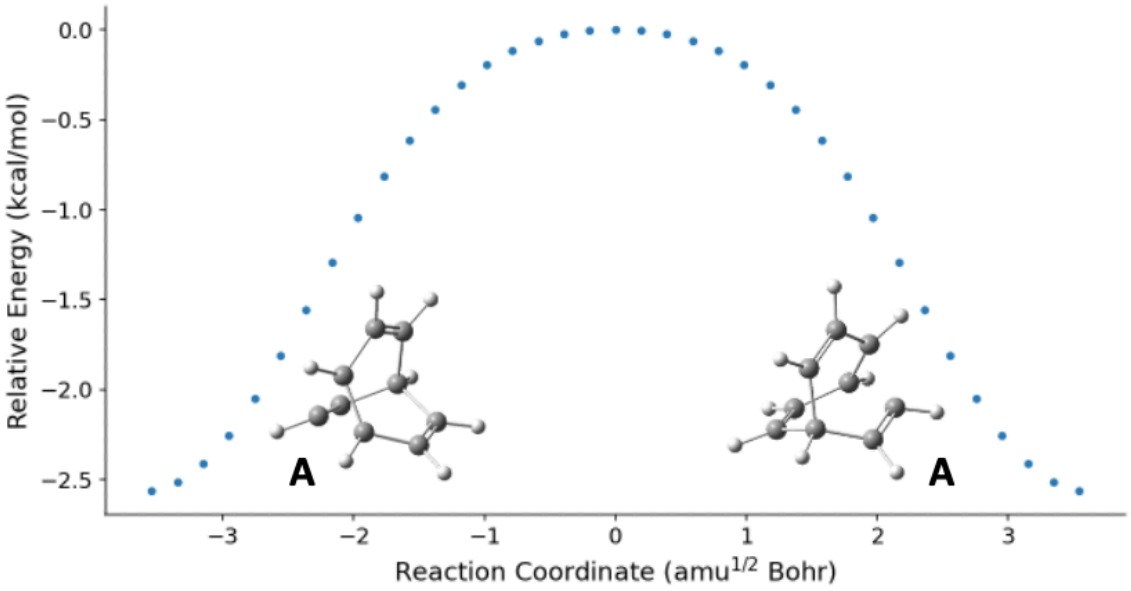
0.0
−0.5
−1.0
−1.5
−2.0
−2.5
Relative Energy (kcal/mol)
−3
−2
−1
0
1
2
3
Reaction Coordinate (amu1/2 Bohr)
A
A

TS3

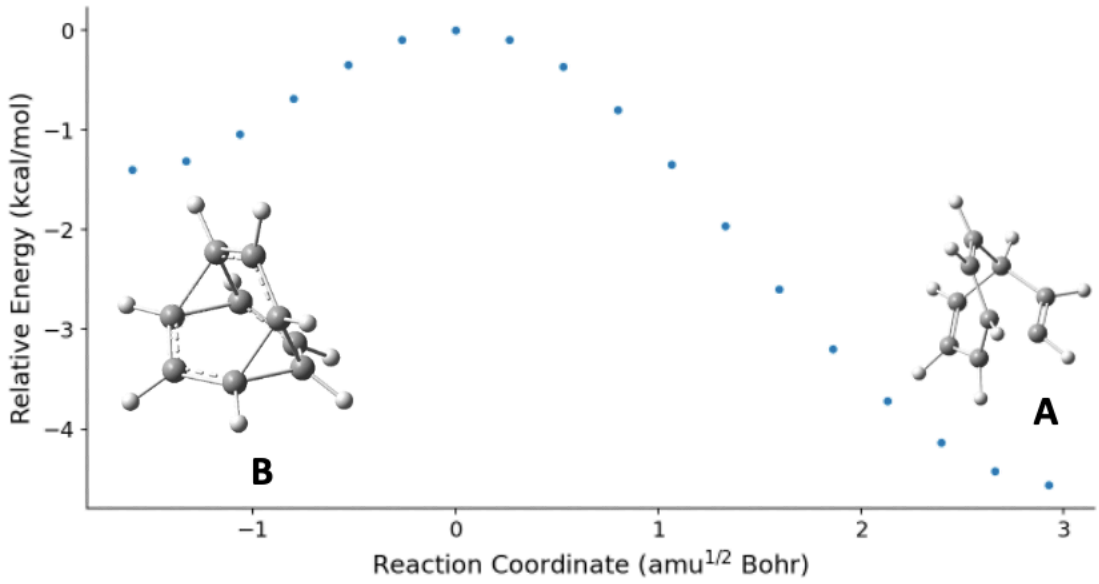
0
−1
−2
−3
−4
Relative Energy (kcal/mol)
−1
0
1
2
3
Reaction Coordinate (amu1/2 Bohr)
B
A

TS4

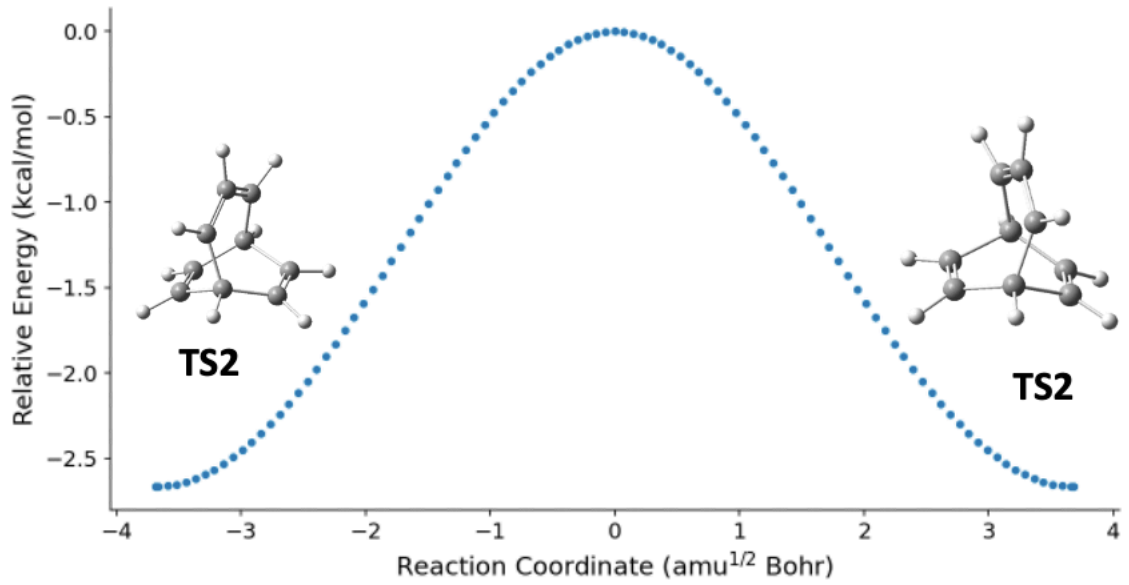
Relative Energy (kcal/mol)
0.0
−0.5
−1.0
−1.5
−2.0
−2.5
−4
−3
−2
−1
0
1
2
3
4
Reaction Coordinate (amu1/2 Bohr)
TS2
TS2

TS5

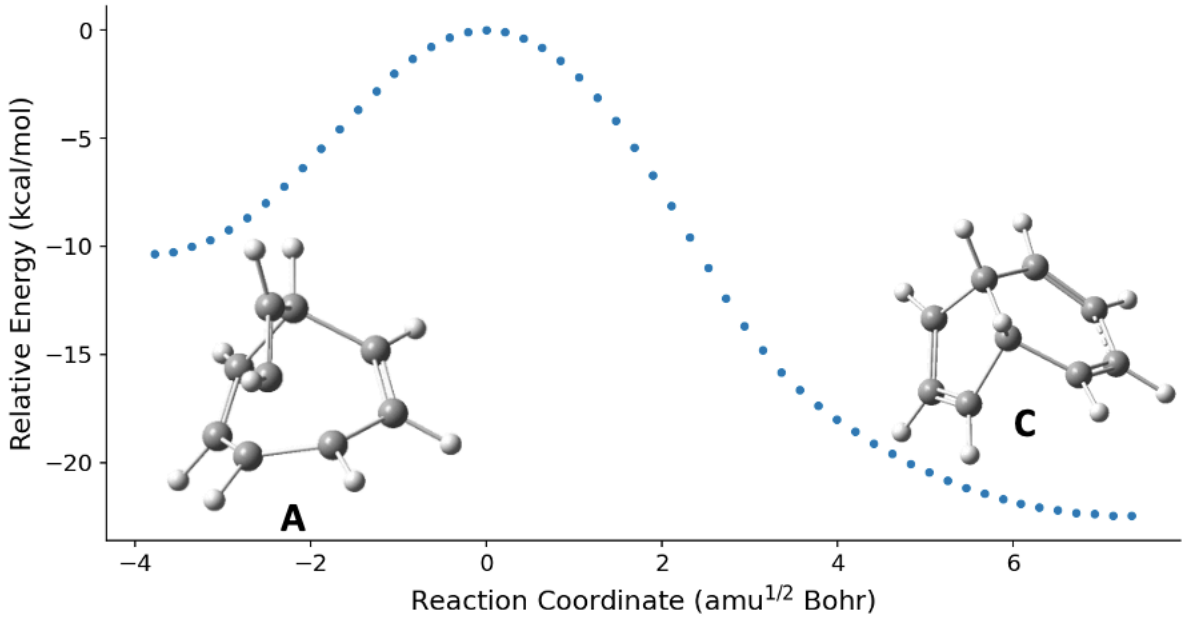
Relative Energy (kcal/mol)
0
−5
−10
−15
−20
−4
−2
0
2
4
6
Reaction Coordinate (amu1/2 Bohr)
A
C

TS6

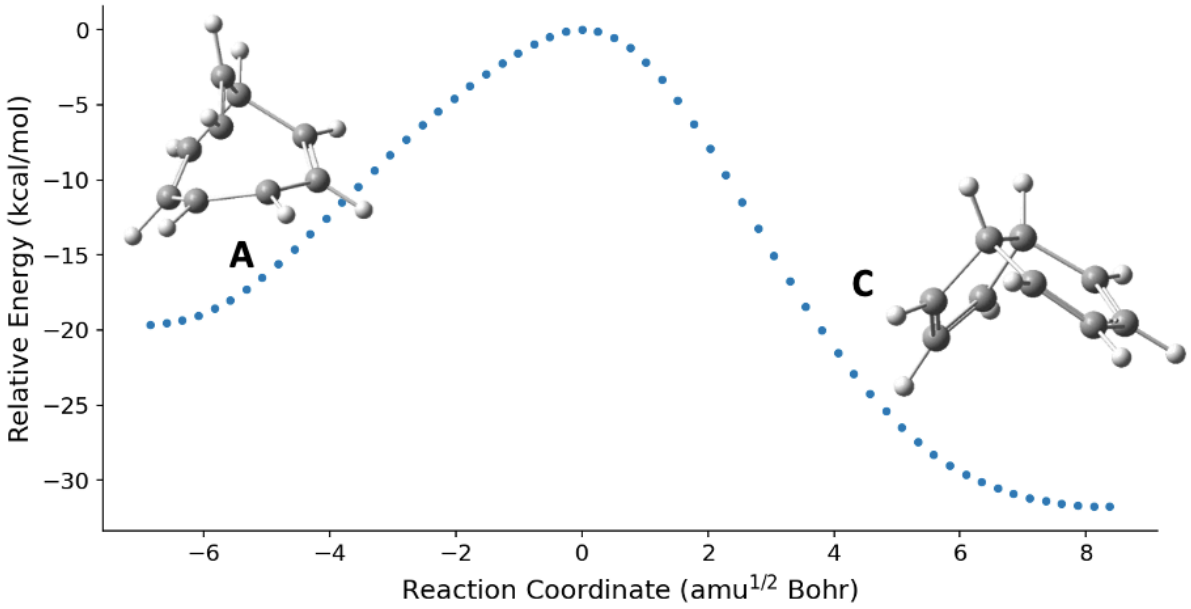
Relative Energy (kcal/mol)
0
−5
−10
−15
−20
−25
−30
A
C
−6
−4
−2
0
2
4
6
8
Reaction Coordinate (amu1/2 Bohr)

TS7

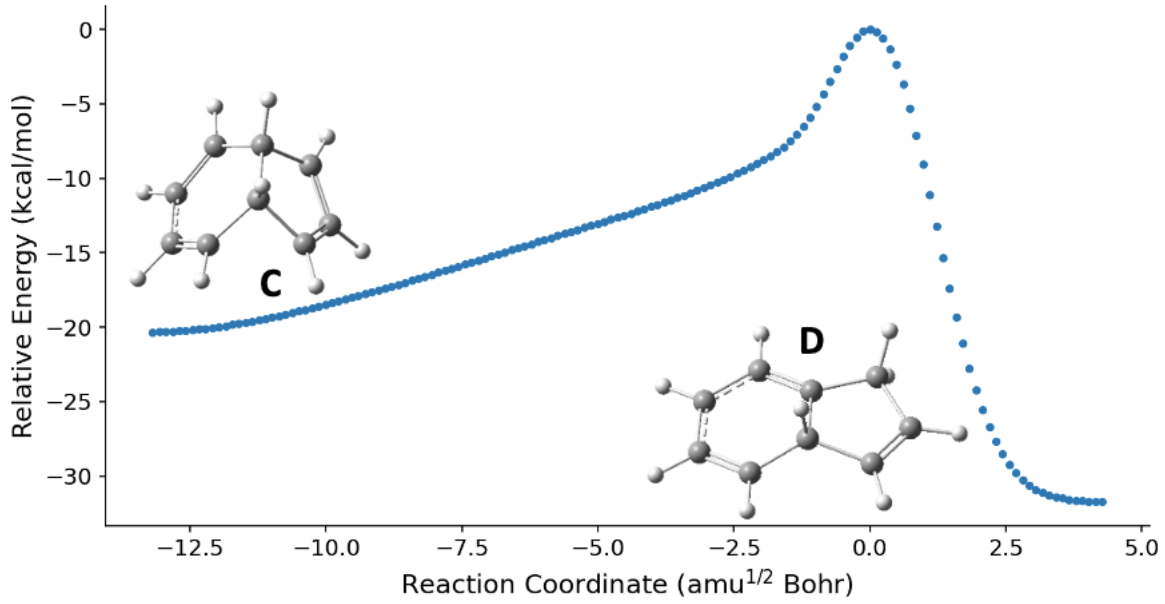
Relative Energy (kcal/mol)
0
−5
−10
−15
−20
−25
−30
C
D
−12.5
−10.0
−7.5
−5.0
−2.5
0.0
2.5
5.0
Reaction Coordinate (amu1/2 Bohr)

TS8

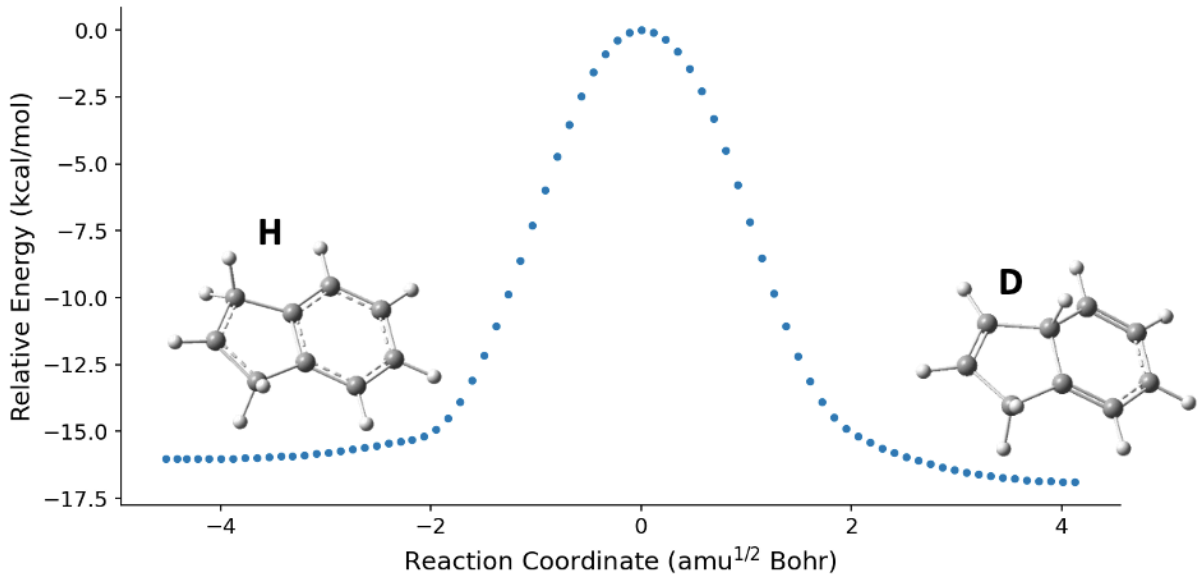
0.0
−2.5
−5.0
−7.5
−10.0
−12.5
−15.0
−17.5
Relative Energy (kcal/mol)
H
D
−4
−2
0
2
4
Reaction Coordinate (amu1/2 Bohr)

TS9

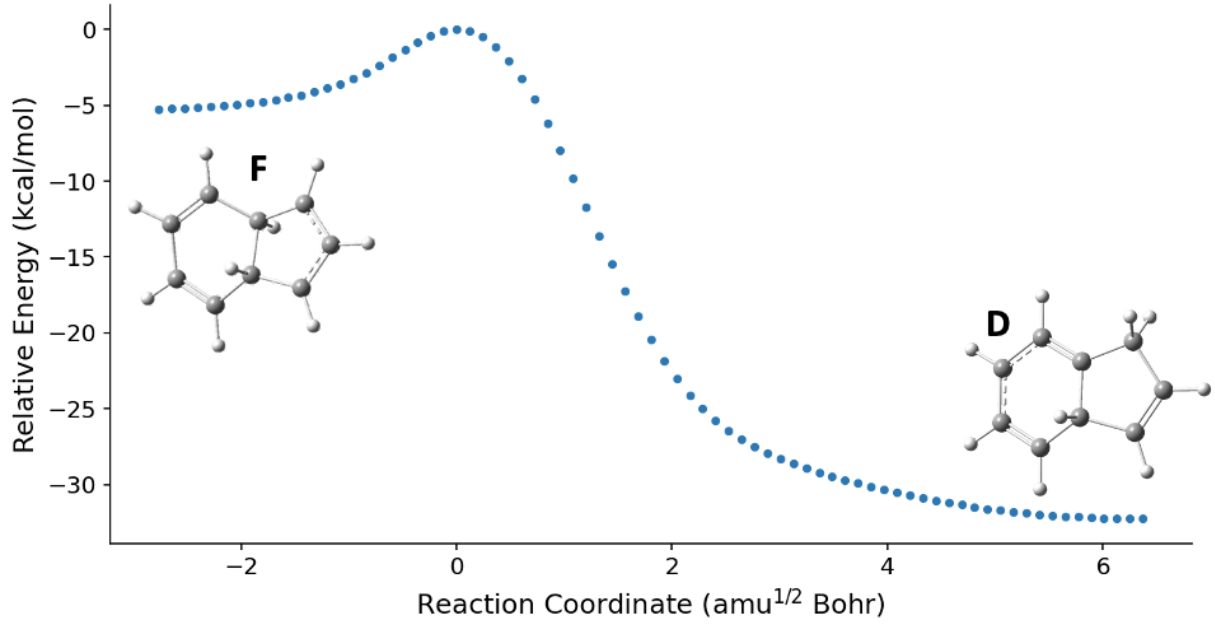
0
−5
−10
−15
−20
−25
−30
Relative Energy (kcal/mol)
F
D
−2
0
2
4
6
Reaction Coordinate (amu1/2 Bohr)

TS10

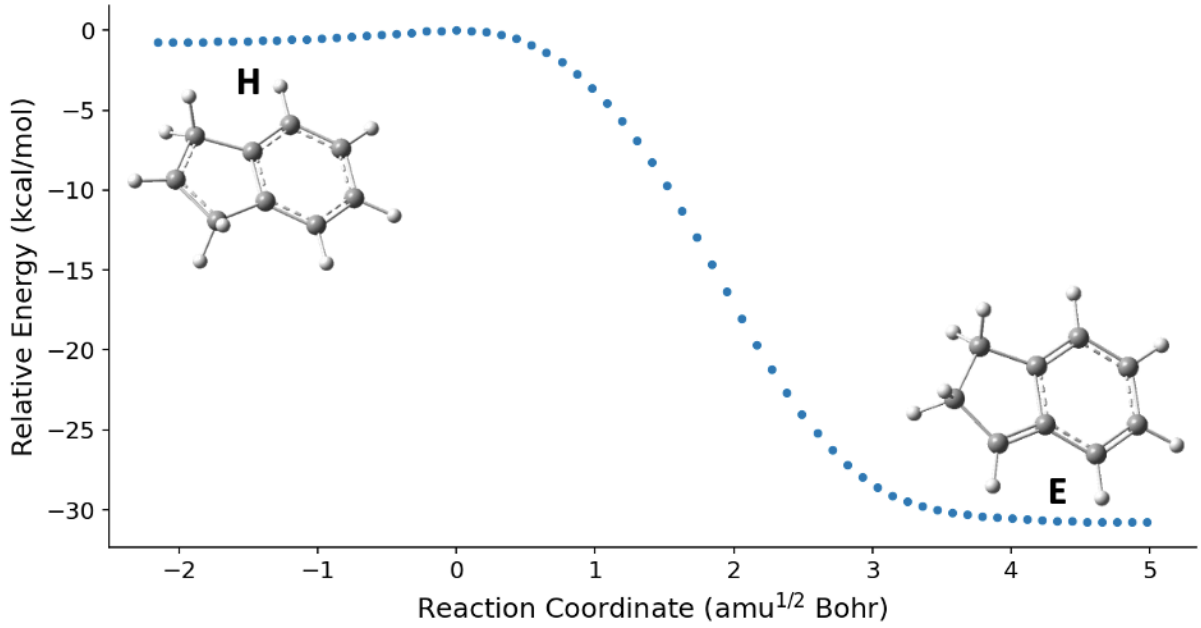
H
E
Relative Energy (kcal/mol)
Reaction Coordinate (amu$^{1/2}$ Bohr)

TS11

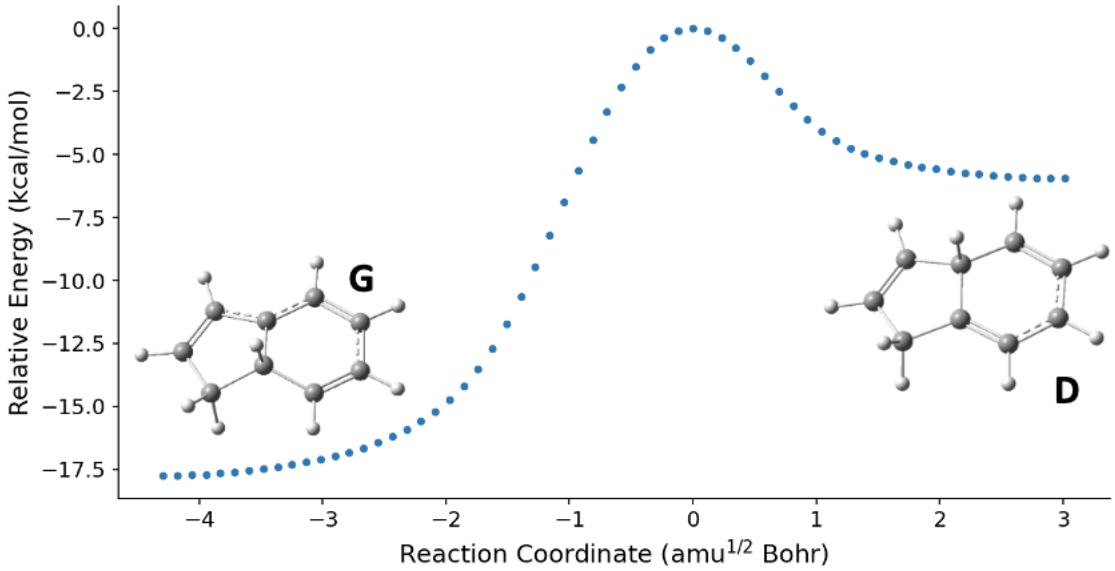
G
D
Relative Energy (kcal/mol)
Reaction Coordinate (amu$^{1/2}$ Bohr)

TS12

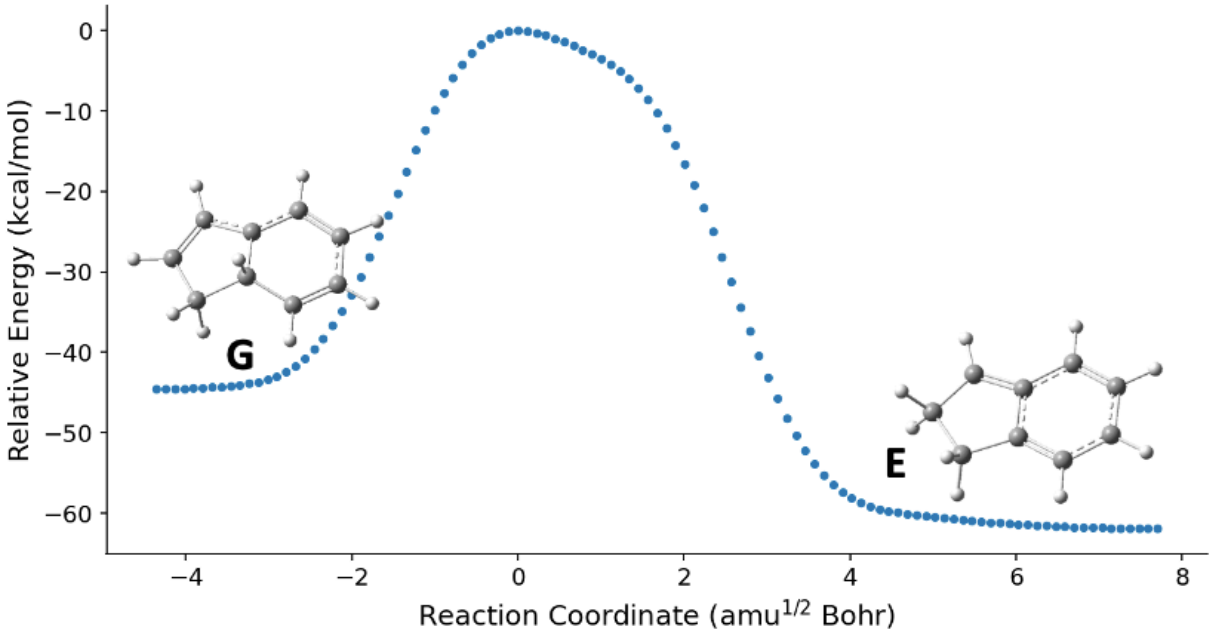
0
−10
−20
−30
−40
−50
−60
Relative Energy (kcal/mol)
G
E
−4
−2
0
2
4
6
8
Reaction Coordinate (amu1/2 Bohr)

Cartesian Coordinates

The output files can be accessed through https://doi.org/10.19061/iochem-bd-6-375

H_2O

O	0.000000	0.000000	0.125364
H	0.000000	0.762039	-0.469369
H	0.000000	-0.762039	-0.469369

Reactant

C	-1.860463	-0.194749	-0.757702
C	-1.514206	0.615999	0.492199
C	0.357674	-1.141568	-0.428841
C	-0.942486	-1.028124	-1.221408
H	-2.825766	-0.047864	-1.228784
H	-1.072570	-1.635463	-2.109380
C	-0.863448	-0.315582	1.509053
H	-1.178892	-0.271263	2.546445
C	0.038644	-1.182387	1.060495
H	0.496969	-1.940509	1.689502
H	0.925352	-2.021955	-0.736473
H	-2.405320	1.080217	0.914665
C	1.199393	0.095291	-0.734901
H	1.745089	0.016312	-1.675200
C	-0.526304	1.695213	0.088842
H	-0.832491	2.729640	0.219668
C	0.664312	1.452872	-0.469751
H	1.281306	2.284826	-0.801539
O	2.454262	-0.084701	0.293994
H	3.046005	0.695946	0.289769
H	2.038242	-0.152182	1.187253

INT

C	-1.909409	-0.317447	-0.756206
C	-1.664421	0.637471	0.389908
C	0.358753	-1.122611	-0.256250
C	-0.929667	-1.130926	-1.132049
H	-2.891073	-0.335055	-1.217168
H	-0.973137	-1.810952	-1.973674
C	-0.968804	-0.140784	1.535486
H	-1.283879	0.058295	2.552756
C	-0.006413	-0.984242	1.195440
H	0.525200	-1.597491	1.913904
H	0.978696	-1.991970	-0.463897
H	-2.587729	1.101996	0.733231
C	0.887201	0.078912	-0.917392
H	1.564169	-0.077187	-1.751239
C	-0.622797	1.675358	0.103112
H	-0.808223	2.689297	0.448053

C	0.517585	1.395731	-0.583800
H	1.165082	2.201498	-0.914354
O	3.072773	-0.087902	0.289754
H	3.930580	-0.386785	-0.047098
H	3.284834	0.453114	1.064168

A

C	-0.015288	-1.307031	0.729931
C	-0.015288	-1.307031	-0.729931
C	-1.362613	-0.708740	0.000000
H	-0.259517	-2.251777	1.207343
H	-0.259517	-2.251777	-1.207343
H	-2.242094	-1.338973	0.000000
C	-1.412791	0.649967	0.000000
H	-2.364949	1.173923	0.000000
C	-0.147683	1.415385	0.000000
H	-0.311829	2.491326	0.000000
C	0.740616	0.963531	1.169035
H	1.364449	1.713555	1.641037
C	0.745981	-0.324306	1.506360
H	1.333246	-0.696628	2.339233
C	0.740616	0.963531	-1.169035
H	1.364449	1.713555	-1.641037
C	0.745981	-0.324306	-1.506360
H	1.333246	-0.696628	-2.339233

B

C	0.000000	1.631741	0.000000
H	0.000000	2.715869	0.000000
C	0.000000	0.920082	1.200483
C	0.000000	0.920082	-1.200483
H	0.000000	1.428562	-2.157046
H	0.000000	1.428562	2.157046
C	1.413128	-0.815874	0.000000
H	2.352006	-1.357947	0.000000
C	0.796793	-0.460033	1.200476
C	0.796793	-0.460033	-1.200476
H	1.237139	-0.714280	-2.157042
H	1.237139	-0.714280	2.157042
C	-1.413128	-0.815874	0.000000
H	-2.352006	-1.357947	0.000000
C	-0.796793	-0.460033	1.200476
C	-0.796793	-0.460033	-1.200476
H	-1.237139	-0.714280	-2.157042
H	-1.237139	-0.714280	2.157042

C

C	0.299755	-1.738855	0.711734
C	0.299755	-1.738855	-0.711734
C	-0.309100	-0.750952	-1.420468
C	-0.882830	0.481245	-0.774022
C	-0.882830	0.481245	0.774022

C	-0.309100	-0.750952	1.420468
H	0.732890	-2.582802	-1.238532
H	0.732890	-2.582802	1.238532
H	-1.809143	0.818509	-1.240794
H	-1.809143	0.818509	1.240794
H	-0.376410	-0.814895	2.501679
H	-0.376410	-0.814895	-2.501679
C	0.347744	1.242060	-1.126816
H	0.620775	1.493121	-2.146062
C	0.347744	1.242060	1.126816
H	0.620775	1.493121	2.146062
C	1.086103	1.565144	0.000000
H	2.050957	2.056586	0.000000

D

C	-2.121270	0.748098	-0.097691
C	-0.917919	1.450076	0.029474
C	0.244237	0.725964	0.137133
C	0.206266	-0.738752	0.288567
C	-1.068993	-1.410136	0.007734
C	-2.203073	-0.662660	-0.125413
H	-3.040108	1.316359	-0.216497
H	-0.908145	2.532419	-0.042142
H	-1.104337	-2.495572	0.023134
H	-3.167505	-1.137315	-0.265004
H	0.159469	-0.833527	1.412600
H	1.792864	1.862570	-0.815686
C	1.595945	-1.200144	-0.090793
H	1.868997	-2.244222	-0.175750
C	1.670190	1.157925	0.016943
H	2.007687	1.698866	0.913659
C	2.401685	-0.145845	-0.192646
H	3.465487	-0.187433	-0.392095

E

C	0.624825	-1.679726	0.000000
C	1.939803	-1.302100	0.000000
C	2.283114	0.071300	0.000000
C	1.336707	1.092710	0.000000
C	0.000881	0.737049	0.000000
C	-0.360412	-0.650519	0.000000
H	0.330946	-2.724136	0.000000
H	2.729152	-2.044895	0.000000
H	3.336360	0.336711	0.000000
H	1.648361	2.131422	0.000000
C	-1.227810	1.590368	0.000000
H	-1.252085	2.246967	0.876478
H	-1.252085	2.246967	-0.876478
C	-1.731481	-0.748236	0.000000
H	-2.284886	-1.684459	0.000000
C	-2.385899	0.575845	0.000000
H	-3.051087	0.666066	-0.870340

H -3.051087   0.666066   0.870340

F
C   0.001086   0.734335 -2.120567
C   0.156455   1.454378 -0.997287
C   0.392476   0.659110   0.247712
C -0.392476 -0.659110   0.247712
C -0.156455 -1.454378 -0.997287
C -0.001086 -0.734335 -2.120567
H -0.109751   1.240264 -3.073928
H   0.206854   2.537319 -0.996871
H -0.206854 -2.537319 -0.996871
H   0.109751 -1.240264 -3.073928
H -1.458668 -0.334422   0.184732
H   1.458668   0.334422   0.184732
C -0.359706 -1.070968   1.654706
H -0.629340 -2.059501   2.017521
C   0.359706   1.070968   1.654706
H   0.629340   2.059501   2.017521
C   0.000000   0.000000   2.464712
H   0.000000   0.000000   3.547381

G
C   2.163018 -0.696715 -0.143370
C   1.026748 -1.412285   0.031701
C -0.236617 -0.713125   0.346903
C -0.236405   0.757164   0.147116
C   0.960327   1.460657   0.043610
C   2.125510   0.731641 -0.106455
H   3.112863 -1.192267 -0.308045
H   1.041566 -2.498049   0.051121
H   0.971770   2.543068 -0.018608
H   3.060225   1.268748 -0.242927
H -0.278133 -0.814467   1.454523
H -1.570613 -1.566097 -1.162188
C -1.586045   1.206763   0.007939
H -1.892165   2.245184 -0.013752
C -1.635738 -1.162118 -0.145209
H -2.112153 -1.927881   0.473490
C -2.389550   0.129260 -0.155473
H -3.466111   0.172749 -0.283971

H
C   2.181667 -0.688213   0.032148
C   0.992487 -1.410133   0.028557
C -0.197690 -0.699938   0.006545
C -0.203507   0.698252 -0.011492
C   0.980715   1.418661 -0.007934
C   2.175860   0.706996   0.014152
H   3.127659 -1.218263   0.049197
H   1.004670 -2.495067   0.042636
H   0.983863   2.503661 -0.021846

H	3.117407	1.245163	0.017426
H	-1.943274	1.831321	0.812836
H	-1.909515	-1.847880	-0.854885
C	-1.625270	1.187892	-0.033175
H	-1.924716	1.809156	-0.902220
C	-1.615328	-1.201785	-0.002317
H	-1.928045	-1.825646	0.860169
C	-2.437128	-0.010458	-0.026542
H	-3.526087	-0.015139	-0.038262

TS1

C	-1.919362	-0.308934	-0.714092
C	-1.591662	0.637444	0.438696
C	0.343258	-1.146850	-0.314514
C	-0.981499	-1.151704	-1.112313
H	-2.911087	-0.272133	-1.150699
H	-1.087113	-1.850637	-1.933098
C	-0.901406	-0.179877	1.543701
H	-1.201584	-0.020562	2.573130
C	0.031349	-1.038829	1.166012
H	0.564145	-1.686600	1.853512
H	0.938417	-2.029221	-0.546232
H	-2.493150	1.119656	0.815480
C	1.011542	0.063757	-0.860243
H	1.650478	-0.091579	-1.725354
C	-0.594323	1.681179	0.015484
H	-0.852255	2.724523	0.181090
C	0.579227	1.400234	-0.598011
H	1.198268	2.210504	-0.969853
O	2.747296	-0.075469	0.299497
H	3.547737	0.344698	-0.058733
H	2.594225	0.329175	1.169958

TS1B

C	-1.902796	-0.317648	-0.787293
C	-1.729736	0.628376	0.371834
C	0.350036	-1.117877	-0.181915
C	-0.883094	-1.100492	-1.140877
H	-2.862181	-0.359755	-1.292321
H	-0.874662	-1.760623	-1.998990
C	-1.066998	-0.139585	1.539442
H	-1.418089	0.060275	2.544841
C	-0.077815	-0.971184	1.243659
H	0.435127	-1.564419	1.992088
H	0.982442	-1.980924	-0.375849
H	-2.675953	1.074291	0.674825
C	0.811232	0.075760	-0.889628
H	1.463787	-0.084901	-1.741347
C	-0.687455	1.686936	0.126960
H	-0.882357	2.690834	0.492419
C	0.453867	1.404045	-0.539697
H	1.131070	2.195189	-0.844607

O	3.131974	0.056636	0.159500
H	3.986311	-0.197434	-0.219727
H	3.355990	0.528371	0.974627

TS2

C	0.000000	0.000000	1.764831
H	0.000000	0.000000	2.851122
C	0.339543	1.158556	1.093641
C	-0.339543	-1.158556	1.093641
H	-0.848178	-1.962458	1.619901
H	0.848178	1.962458	1.619901
C	-1.221160	0.693086	-0.849432
H	-2.018948	1.294754	-1.271179
C	0.000000	1.386626	-0.333365
C	-1.280195	-0.634915	-0.807994
H	-2.140813	-1.229279	-1.088984
H	0.042387	2.441799	-0.596890
C	1.221160	-0.693086	-0.849432
H	2.018948	-1.294754	-1.271179
C	1.280195	0.634915	-0.807994
C	0.000000	-1.386626	-0.333365
H	-0.042387	-2.441799	-0.596890
H	2.140813	1.229279	-1.088984

TS3

C	0.036695	-1.298476	0.758770
C	0.036695	-1.298476	-0.758770
C	-1.311252	-0.789867	0.000000
H	-0.095088	-2.270931	1.219363
H	-0.095088	-2.270931	-1.219363
H	-2.133052	-1.494579	0.000000
C	-1.509924	0.570504	0.000000
H	-2.509883	0.990092	0.000000
C	-0.368158	1.429885	0.000000
H	-0.538999	2.501456	0.000000
C	0.784511	0.980791	0.923200
H	1.418237	1.770063	1.307842
C	0.768042	-0.287406	1.432800
H	1.332088	-0.535315	2.324671
C	0.784511	0.980791	-0.923200
H	1.418237	1.770063	-1.307842
C	0.768042	-0.287406	-1.432800
H	1.332088	-0.535315	-2.324671

TS4

C	1.241402	0.657702	-0.888730
C	0.000000	1.372930	-0.311528
C	0.000000	-1.372930	-0.311528
C	1.241402	-0.657702	-0.888730
H	2.039462	1.276972	-1.281032
H	2.039462	-1.276972	-1.281032
C	0.000000	1.212191	1.158637

H	0.000000	2.116154	1.766290
C	0.000000	-1.212191	1.158637
H	0.000000	-2.116154	1.766290
H	0.000000	-2.429780	-0.574418
H	0.000000	2.429780	-0.574418
C	-1.241402	-0.657702	-0.888730
H	-2.039462	-1.276972	-1.281032
C	-1.241402	0.657702	-0.888730
H	-2.039462	1.276972	-1.281032
C	0.000000	0.000000	1.828893
H	0.000000	0.000000	2.913426

TS5

C	1.252832	0.880936	-0.030123
C	1.345216	-0.604115	-0.380820
C	0.992068	-0.234341	1.032077
H	2.216036	1.372861	0.054170
H	2.348612	-0.978271	-0.550257
H	1.708070	-0.417165	1.824107
C	-0.407785	-0.511204	1.280581
H	-0.703944	-1.147893	2.110143
C	-1.404428	0.041037	0.424258
H	-2.430414	-0.112185	0.749787
C	-1.136229	1.314055	-0.282252
H	-1.985354	1.881280	-0.644719
C	0.126659	1.715472	-0.452360
H	0.354017	2.664389	-0.926299
C	-1.006135	-1.214622	-0.534243
H	-1.863911	-1.799384	-0.843384
C	0.225816	-1.301931	-1.047690
H	0.415222	-1.896033	-1.936722

TS6

C	1.412762	0.389552	-0.542768
C	0.536659	-1.157716	-0.429442
C	1.473184	-0.331240	0.688579
H	2.291228	0.375881	-1.178405
H	1.117067	-2.050290	-0.640351
H	2.347910	-0.898901	0.992751
C	0.188661	-0.651446	1.158802
H	0.084826	-1.406576	1.932191
C	-1.012746	0.269416	0.866600
H	-1.619939	0.421989	1.759813
C	-0.574345	1.557499	0.201487
H	-1.233269	2.416841	0.261915
C	0.516290	1.555023	-0.572269
H	0.794528	2.392507	-1.200934
C	-1.713460	-0.414955	-0.288002
H	-2.744115	-0.221739	-0.558621
C	-0.834496	-1.115612	-1.000514
H	-1.001900	-1.620468	-1.944292

TS7

C	-2.134010	0.683992	-0.112301
C	-1.038454	1.437954	0.113216
C	0.233546	0.750030	0.210745
C	0.286286	-0.748863	0.397168
C	-0.961479	-1.458617	-0.043616
C	-2.092432	-0.767830	-0.230644
H	-3.088389	1.179253	-0.259935
H	-1.075088	2.521291	0.121710
H	-0.933839	-2.541834	-0.093881
H	-3.010831	-1.286360	-0.481882
H	0.306864	-0.943923	1.493048
H	1.815895	2.185388	-0.390778
C	1.671597	-1.111847	-0.032591
H	2.050749	-2.127298	-0.017784
C	1.541325	1.157613	-0.170258
H	0.985924	1.258234	1.102945
C	2.399373	0.000270	-0.274187
H	3.453864	0.051921	-0.509743

TS8

C	2.173824	-0.716232	-0.017107
C	0.977984	-1.429703	0.014996
C	-0.208668	-0.718376	0.030782
C	-0.167109	0.696320	0.008147
C	1.035378	1.421117	-0.002004
C	2.204629	0.686572	-0.031130
H	3.112176	-1.260638	-0.029372
H	0.983010	-2.514341	0.020208
H	1.043597	2.505685	0.005197
H	3.159535	1.199020	-0.058879
H	-0.951441	1.010955	1.010317
H	-1.837713	-1.708032	-0.948251
C	-1.636432	1.186318	-0.033866
H	-1.919561	2.227105	-0.129697
C	-1.637556	-1.169380	-0.006469
H	-1.933072	-1.865324	0.789031
C	-2.440234	0.084402	-0.038830
H	-3.520325	0.107160	-0.122404

TS9

C	-2.150424	0.679998	0.050048
C	-1.041298	1.442816	0.160325
C	0.232166	0.747919	-0.000469
C	0.265317	-0.727356	0.304879
C	-0.966631	-1.459582	-0.120972
C	-2.109525	-0.758316	-0.192546
H	-3.124487	1.153065	0.122724
H	-1.082065	2.519838	0.274918
H	-0.937016	-2.535180	-0.255742
H	-3.042369	-1.260911	-0.422968
H	0.210480	-0.732826	1.418806

H	0.572845	0.881753	-1.161460
C	1.687509	-1.111736	0.091376
H	2.050938	-2.132449	0.128658
C	1.594175	1.152453	-0.120673
H	1.918301	2.182025	-0.245951
C	2.447617	-0.003803	-0.099846
H	3.519251	0.033517	-0.243160

TS10

C	2.208899	-0.705641	-0.022311
C	1.022167	-1.428902	-0.042514
C	-0.166105	-0.712961	-0.041471
C	-0.181139	0.687759	-0.016000
C	1.003590	1.405138	0.013326
C	2.198302	0.690394	0.009553
H	3.156649	-1.232520	-0.029302
H	1.031200	-2.513575	-0.060859
H	1.009058	2.489915	0.033339
H	3.139705	1.228716	0.029042
H	-1.924552	1.887199	0.716800
H	-1.900584	-2.172318	-0.373533
C	-1.605904	1.173329	-0.055489
H	-1.858052	1.686693	-1.007758
C	-1.574487	-1.192727	-0.020577
H	-1.948621	-1.160085	1.083361
C	-2.415149	-0.048435	-0.097287
H	-3.502083	-0.081674	-0.117703

TS11

C	2.159125	-0.721318	-0.042418
C	0.978799	-1.429158	0.016815
C	-0.231726	-0.712332	0.060486
C	-0.218289	0.739562	0.082028
C	1.031117	1.431999	-0.013703
C	2.185860	0.695861	-0.058645
H	3.099767	-1.260967	-0.080186
H	0.970660	-2.513468	0.006503
H	1.046044	2.515862	-0.043674
H	3.143336	1.201962	-0.117306
H	-0.142716	0.163202	1.171268
H	-1.805500	-1.748450	-0.928460
C	-1.619860	1.205848	-0.032534
H	-1.901544	2.250174	-0.050892
C	-1.666682	-1.153850	-0.015248
H	-1.973082	-1.799316	0.816811
C	-2.429437	0.143275	-0.076816
H	-3.510667	0.176094	-0.129813

TS12

C	2.132879	-0.741100	-0.152472
C	0.997948	-1.452847	-0.058591
C	-0.252757	-0.719648	0.262106

C	-0.236913	0.775895	0.107141
C	1.032105	1.447580	0.094384
C	2.157520	0.708692	-0.032207
H	3.071918	-1.253282	-0.333225
H	0.983483	-2.535045	-0.124913
H	1.064990	2.530967	0.122236
H	3.121103	1.204283	-0.083215
H	-0.395862	-0.860020	1.380599
H	-2.237983	-0.418273	-1.200591
C	-1.509099	1.225139	-0.056125
H	-1.836305	2.249549	-0.169478
C	-1.642792	-1.122487	0.051350
H	-2.043906	-2.130205	0.073826
C	-2.406196	0.070781	-0.127295
H	-3.484544	0.113553	0.011749

Reference

(1) Zhao, Y.; Truhlar, D. G. The M06 Suite of Density Functionals for Main Group Thermochemistry, Thermochemical Kinetics, Noncovalent Interactions, Excited States, and Transition Elements: Two New Functionals and Systematic Testing of Four M06-Class Functionals and 12 Other Functionals. *Theor. Chem. Acc.* **2008**, *120* (1), 215–241.

(2) Weigend, F.; Ahlrichs, R. Balanced Basis Sets of Split Valence, Triple Zeta Valence and Quadruple Zeta Valence Quality for H to Rn: Design and Assessment of Accuracy. *Phys. Chem. Chem. Phys.* **2005**, *7* (18), 3297–3305.

(3) Riplinger, C.; Sandhoefer, B.; Hansen, A.; Neese, F. Natural Triple Excitations in Local Coupled Cluster Calculations with Pair Natural Orbitals. *J. Chem. Phys.* **2013**, *139* (13), 134101.

(4) Riplinger, C.; Neese, F. An Efficient and near Linear Scaling Pair Natural Orbital Based Local Coupled Cluster Method. *J. Chem. Phys.* **2013**, *138* (3), 034106.

(5) Guo, Y.; Riplinger, C.; Becker, U.; Liakos, D. G.; Minenkov, Y.; Cavallo, L.; Neese, F. Communication: An Improved Linear Scaling Perturbative Triples Correction for the Domain Based Local Pair-Natural Orbital Based Singles and Doubles Coupled Cluster Method [DLPNO-CCSD(T)]. *J. Chem. Phys.* **2018**, *148* (1), 011101.

(6) Luchini, G.; Alegre-Requena, J. V.; Funes-Ardoiz, I.; Paton, R. S. GoodVibes: Automated Thermochemistry for Heterogeneous Computational Chemistry Data. *F1000Res.* **2020**, *9*, 291.

(7) Cremer, D.; Svensson, P.; Kraka, E.; Ahlberg, P. Exploration of the Potential Energy Surface of C9H9+ by Ab Initio Methods. 1. The Barbaralyl Cation. *J. Am. Chem. Soc.* **1993**, *115* (16), 7445–7456.

(8) Werstiuk, N. H. The 9-Barbaralyl and Related C9H9+ Carbocations — A QTAIM-DI-VISAB Computational Study. *Can. J. Chem.* **2010**, *88* (11), 1195–1204.

(9) Ditchfield, R.; Hehre, W. J.; Pople, J. A. Self-Consistent Molecular-Orbital Methods. IX. An Extended Gaussian-Type Basis for Molecular-Orbital Studies of Organic Molecules. *J. Chem. Phys.* **1971**, *54* (2), 724–728.

(10) Yanai, T.; Tew, D. P.; Handy, N. C. A New Hybrid Exchange–Correlation Functional Using the Coulomb-Attenuating Method (CAM-B3LYP). *Chem. Phys. Lett.* **2004**, *393* (1–3), 51–57.

(11) Fukui, K. The Path of Chemical Reactions - the IRC Approach. *Acc. Chem. Res.* **1981**, *14* (12), 363–368.

(12) Álvarez-Moreno, M.; de Graaf, C.; López, N.; Maseras, F.; Poblet, J. M.; Bo, C. Managing the Computational Chemistry Big Data Problem: The IoChem-BD Platform. *J. Chem. Inf. Model.* **2015**, *55* (1), 95–103.

(13) Chai, J.-D.; Head-Gordon, M. Long-Range Corrected Hybrid Density Functionals with Damped Atom-Atom Dispersion Corrections. *Phys. Chem. Chem. Phys.* **2008**, *10* (44), 6615–6620.

(14) Austin, A.; Petersson, G. A.; Frisch, M. J.; Dobek, F. J.; Scalmani, G.; Throssell, K. A Density Functional with Spherical Atom Dispersion Terms. *J. Chem. Theory Comput.* **2012**, *8* (12), 4989–5007.

(15) Becke, A. D. Density-Functional Thermochemistry. IV. A New Dynamical Correlation Functional and Implications for Exact-Exchange Mixing. *J. Chem. Phys.* **1996**, *104* (3), 1040–1046.

(16) Adamo, C.; Barone, V. Toward Reliable Adiabatic Connection Models Free from Adjustable Parameters. *Chem. Phys. Lett.* **1997**, *274* (1–3), 242–250.
(17) Becke, A. D. Density-Functional Thermochemistry. III. The Role of Exact Exchange. *J. Chem. Phys.* **1993**, *98* (7), 5648–5652.
(18) Grimme, S.; Ehrlich, S.; Goerigk, L. Effect of the Damping Function in Dispersion Corrected Density Functional Theory. *J. Comput. Chem.* **2011**, *32* (7), 1456–1465.
(19) Grimme, S. Semiempirical GGA-Type Density Functional Constructed with a Long-Range Dispersion Correction. *J. Comput. Chem.* **2006**, *27* (15), 1787–1799.
(20) Becke, A. D. A New Mixing of Hartree-Fock and Local Density-Functional Theories. *J. Chem. Phys.* **1993**, *98*, 1372–1377.
(21) Becke, A. D. Density-Functional Exchange-Energy Approximation with Correct Asymptotic Behavior. *Phys. Rev. A Gen. Phys.* **1988**, *38* (6), 3098–3100.
(22) Lee, C.; Yang, W.; Parr, R. G. Development of the Colle-Salvetti Correlation-Energy Formula into a Functional of the Electron Density. *Phys. Rev. B Condens. Matter* **1988**, *37* (2), 785–789.
(23) Miehlich, B.; Savin, A.; Stoll, H.; Preuss, H. Results Obtained with the Correlation Energy Density Functionals of Becke and Lee, Yang and Parr. *Chem. Phys. Lett.* **1989**, *157* (3), 200–206.
(24) Boese, A. D.; Martin, J. M. L. Development of Density Functionals for Thermochemical Kinetics. *J. Chem. Phys.* **2004**, *121* (8), 3405–3416.
(25) Adamo, C.; Barone, V. Toward Reliable Density Functional Methods without Adjustable Parameters: The PBE0 Model. *J. Chem. Phys.* **1999**, *110* (13), 6158–6170.
(26) Ernzerhof, M.; Scuseria, G. E. Assessment of the Perdew–Burke–Ernzerhof Exchange-Correlation Functional. *J. Chem. Phys.* **1999**, *110* (11), 5029–5036.
(27) Izmaylov, A. F.; Scuseria, G. E.; Frisch, M. J. Efficient Evaluation of Short-Range Hartree-Fock Exchange in Large Molecules and Periodic Systems. *J. Chem. Phys.* **2006**, *125* (10), 104103.
(28) Iikura, H.; Tsuneda, T.; Yanai, T.; Hirao, K. A Long-Range Correction Scheme for Generalized-Gradient-Approximation Exchange Functionals. *J. Chem. Phys.* **2001**, *115* (8), 3540–3544.
(29) Vydrov, O. A.; Scuseria, G. E. Assessment of a Long-Range Corrected Hybrid Functional. *J. Chem. Phys.* **2006**, *125* (23), 234109.
(30) Zhao, Y.; Truhlar, D. G. A New Local Density Functional for Main-Group Thermochemistry, Transition Metal Bonding, Thermochemical Kinetics, and Noncovalent Interactions. *J. Chem. Phys.* **2006**, *125* (19), 194101.
(31) Peverati, R.; Truhlar, D. G. Improving the Accuracy of Hybrid Meta-GGA Density Functionals by Range Separation. *J. Phys. Chem. Lett.* **2011**, *2* (21), 2810–2817.
(32) Peverati, R.; Truhlar, D. G. An Improved and Broadly Accurate Local Approximation to the Exchange-Correlation Density Functional: The MN12-L Functional for Electronic Structure Calculations in Chemistry and Physics. *Phys. Chem. Chem. Phys.* **2012**, *14* (38), 13171–13174.
(33) Peverati, R.; Truhlar, D. G. Screened-Exchange Density Functionals with Broad Accuracy for Chemistry and Solid-State Physics. *Phys. Chem. Chem. Phys.* **2012**, *14* (47), 16187–16191.

(34) Yu, H. S.; He, X.; Li, S. L.; Truhlar, D. G. MN15: A Kohn-Sham Global-Hybrid Exchange-Correlation Density Functional with Broad Accuracy for Multi-Reference and Single-Reference Systems and Noncovalent Interactions. *Chem. Sci.* **2016**, *7* (8), 5032–5051.
(35) Handy, N. C.; Cohen, A. J. Left-Right Correlation Energy. *Mol. Phys.* **2001**, *99* (5), 403–412.
(36) Hoe, W.-M.; Cohen, A. J.; Handy, N. C. Assessment of a New Local Exchange Functional OPTX. *Chem. Phys. Lett.* **2001**, *341* (3–4), 319–328.
(37) Zhao, Y.; Truhlar, D. G. Design of Density Functionals That Are Broadly Accurate for Thermochemistry, Thermochemical Kinetics, and Nonbonded Interactions. *J. Phys. Chem. A* **2005**, *109* (25), 5656–5667.
(38) Peverati, R.; Truhlar, D. G. Communication: A Global Hybrid Generalized Gradient Approximation to the Exchange-Correlation Functional That Satisfies the Second-Order Density-Gradient Constraint and Has Broad Applicability in Chemistry. *J. Chem. Phys.* **2011**, *135* (19), 191102.
(39) Tao, J.; Perdew, J. P.; Staroverov, V. N.; Scuseria, G. E. Climbing the Density Functional Ladder: Nonempirical Meta-Generalized Gradient Approximation Designed for Molecules and Solids. *Phys. Rev. Lett.* **2003**, *91* (14), 146401.
(40) Staroverov, V. N.; Scuseria, G. E.; Tao, J.; Perdew, J. P. Comparative Assessment of a New Nonempirical Density Functional: Molecules and Hydrogen-Bonded Complexes. *J. Chem. Phys.* **2003**, *119* (23), 12129–12137.
(41) Adamo, C.; Barone, V. Exchange Functionals with Improved Long-Range Behavior and Adiabatic Connection Methods without Adjustable Parameters: The m PW and m PW1PW Models. *J. Chem. Phys.* **1998**, *108* (2), 664–675.
(42) Perdew, J. P.; Ruzsinszky, A.; Csonka, G. I.; Constantin, L. A.; Sun, J. Workhorse Semilocal Density Functional for Condensed Matter Physics and Quantum Chemistry. *Phys. Rev. Lett.* **2009**, *103* (2).
(43) Perdew, J. P.; Ruzsinszky, A.; Csonka, G. I.; Constantin, L. A.; Sun, J. Erratum: Workhorse Semilocal Density Functional for Condensed Matter Physics and Quantum Chemistry [Phys. Rev. Lett.103, 026403 (2009)]. *Phys. Rev. Lett.* **2011**, *106* (17). https://doi.org/10.1103/physrevlett.106.179902.
(44) Boese, A. D.; Handy, N. C. New Exchange-Correlation Density Functionals: The Role of the Kinetic-Energy Density. *J. Chem. Phys.* **2002**, *116* (22), 9559–9569.
(45) Chai, J.-D.; Head-Gordon, M. Systematic Optimization of Long-Range Corrected Hybrid Density Functionals. *J. Chem. Phys.* **2008**, *128* (8), 084106.
(46) Zubarev, D. Y.; Boldyrev, A. I. ”Developing Paradigms of Chemical Bonding: Adaptive Natural Density Partitioning. *Phys. Chem. Chem. Phys.* **2008**, *10* (34), 5207.
(47) Lu, T.; Chen, F. Multiwfn: A Multifunctional Wavefunction Analyzer. *J. Comput. Chem.* **2012**, *33* (5), 580–592.